R-06-30

A preliminary investigation of the concept of 'hyper-convergence' using 'sparse' channel networks

J H Black, In Situ Solutions

P C Robinson, Quintessa Ltd

J A Barker, University College London

January 2006

Svensk Kärnbränslehantering AB
Swedish Nuclear Fuel
and Waste Management Co
Box 5864
SE-102 40 Stockholm Sweden
Tel 08-459 84 00
+46 8 459 84 00
Fax 08-661 57 19
+46 8 661 57 19

ISSN 1402-3091
SKB Rapport R-06-30

A preliminary investigation of the concept of 'hyper-convergence' using 'sparse' channel networks

J H Black, In Situ Solutions

P C Robinson, Quintessa Ltd

J A Barker, University College London

January 2006

Executive summary

This report summarises a preliminary investigation of the concept of 'hyper-convergence', a new explanation of why drifts in fractured crystalline rocks usually appear to be surrounded by a 'skin' of reduced hydraulic conductivity (K). The idea (summarised in Figure 1) is that when groundwater flows into a drift in fractured crystalline rock, there are only a limited number of inflow points towards which the inflowing water must converge. This convergence is extra to that which would be expected if the inflow were converging towards a true line source rather than a series of point inflows arranged along a line. The 'extra' convergence is here termed 'hyper-convergence'. It causes 'extra' head loss and is usually perceived as a skin of reduced K. The effect is foreseen to be intimately associated with groundwater flow in **sparse channel** networks.

The investigation is based on developing a numerical model of a 'sparse channel network', using it to simulate inflow into a drift and then comparing the results to detailed measurements of an actual drift at the Stripa Mine, the Macro-Permeability Experiment.

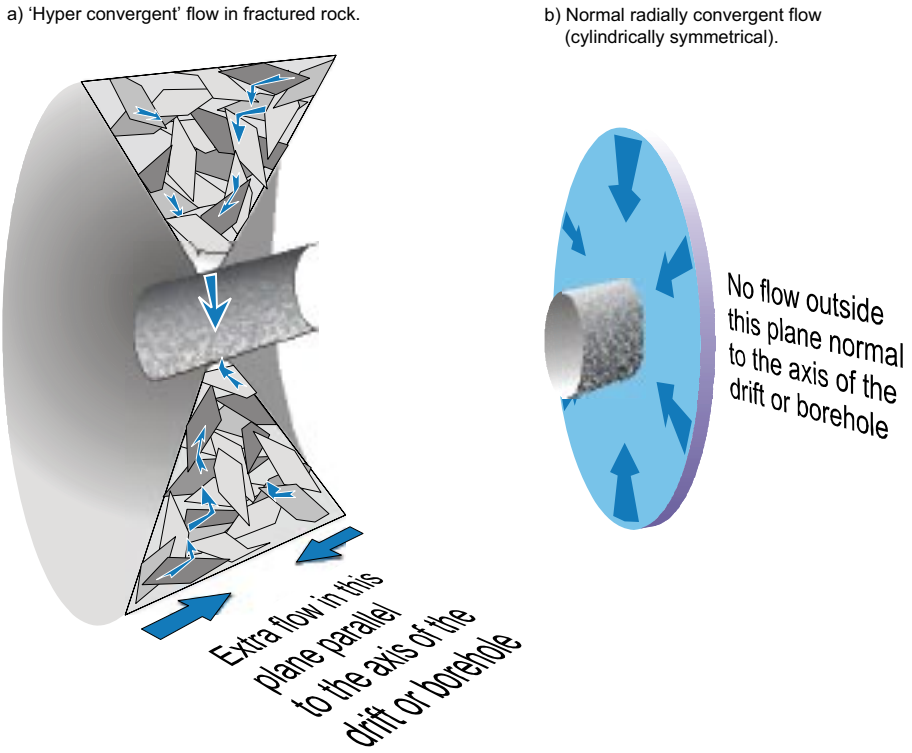

Figure 1. *The concept of hyper-convergent flow towards a drift or borehole.*

A simple, effective and flexible channel network code, named HyperConv, has been devised. After minimal initial experimentation, and using plausible parameters based on a review of some underground experiments at Stripa, some realistic looking results have been produced (Figure 2). They arise from realisations of systems where only 20% or less of nodes of an orthogonal grid are active. Most important to reproducing hyper-convergent behaviour is the length of individual channels. Halving the length and doubling the number of channels (i.e. keeping channel density constant), in the range of systems briefly examined, changed system behaviour radically resulting in negative 'skins' rather than the positive values commonly observed. A more detailed evaluation of 100 realisations of a network designed to be sparse (and therefore hyper-convergent) was undertaken. The more detailed study, which used 4.8% active nodes and a channel conductance chosen from a log normal distribution with a standard deviation of 2 orders of magnitude, yielded some surprising results:

It is concluded that the basic attributes of a sparse channel network are:

- The individual channels are significantly elongated in one direction with aspect ratios in the order of 10:1 or more.
- The highly non-equidimensional channels have a moderate frequency of occurrence but a low chance of interconnection so that the overall network is close to the limit of percolation.

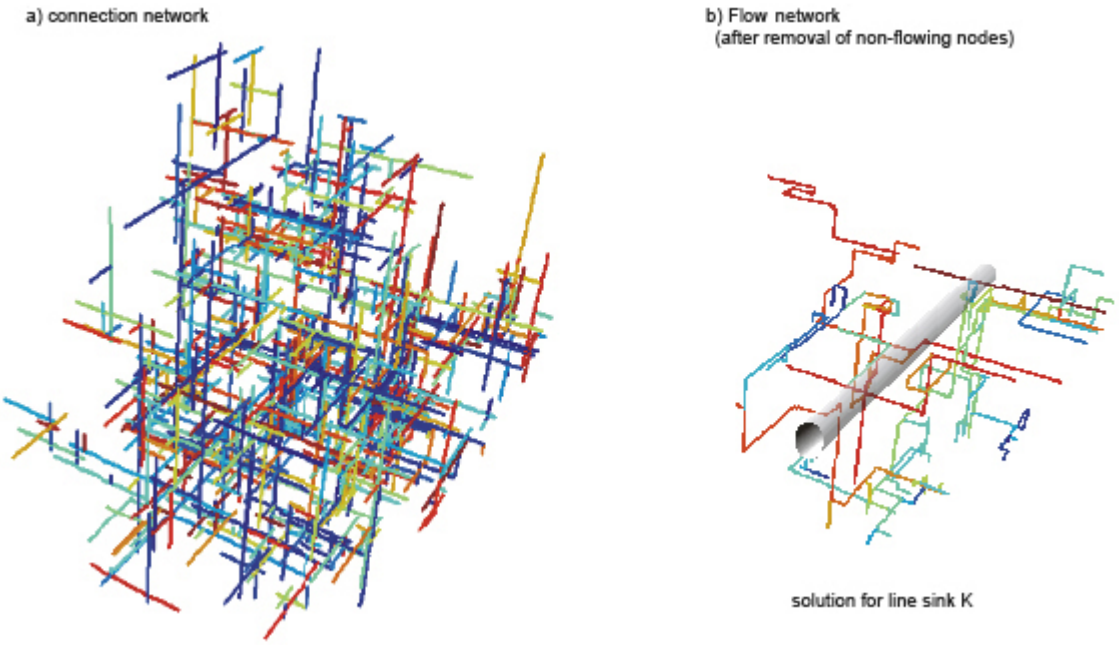

Figure 2. *Example of how a sparse network of connections is reduced to an even sparser flow network. Note that the modelled system is roughly a cylinder of 90 m diameter and the drift is 4 m diameter. Nodes are set at 1.5 m centres and channels average 15 m long (i.e. 10 spacings).*

These basic attributes give rise to a number of characteristic behaviours, of which 'hyper-convergence' around drifts and boreholes is one. The others are also consequences that are observable in field experiments.

The main direct conclusions from the modelling were that:

- There were only a small number of inflow points to the modelled drift.
- There was no direct relationship between derived hydraulic conductivity and skin effect.
- The modelling reproduced the key features of the Macro-Permeability experiment.
- The meaning and validity of the value of hydraulic conductivity derived from a drift inflow experiment are very uncertain.

The modelling included a target hydraulic conductivity ($K_{creation}$) that was used to control the variability of conductances used in model creation. It was effectively an upscaling of the collective small-scale values. Subsequent calculations involved a cylindrical version of the lattice network that produced 3 'drift-scale' values of hydraulic conductivity and a cuboidal version that produced a 'large-scale' value. Thus each realisation of the model was associated with 5 values of hydraulic conductivity. As it turned out, the 'drift-scale' values were all quite similar so that effectively there were 3 values each appropriate to a different length scale: small, medium and 'medium-large'. Each one differed by about a factor of 10. If this reasoning is compared to the field values then it appears that what has been measured are the two smaller scale values and that the true large-scale value for Stripa is another order of magnitude less than previously thought. This would also be the case for other sites where sparse channel networks apply.

The main indirect conclusions from this modelling project are:

- That sparse channel networks can be expected to produce 'hyper-convergence' and that where skin effects are apparently observed then a sparse channel network system should be assumed.
- That sparse channel networks can be expected to produce compartmentalisation in the head regime surrounding any natural or artificial flow system such as an excavation or a mine. This is because a few low conductance connectors are the effective controls on the overall flow system.
- That exploration boreholes into sparse channel networks can be expected to be active participants in the system they are being used to observe
- That EDZs are largely fictitious in terms of altered hydrogeological properties except at the microscopic scale. There is no evidence of an Excavation Damaged Zone of enhanced hydraulic conductivity.

In conclusion, it can be seen that what began as a search for an explanation of a feature of a 20 year old underground experiment turned into a re-appraisal of many concepts that are familiar and well established.

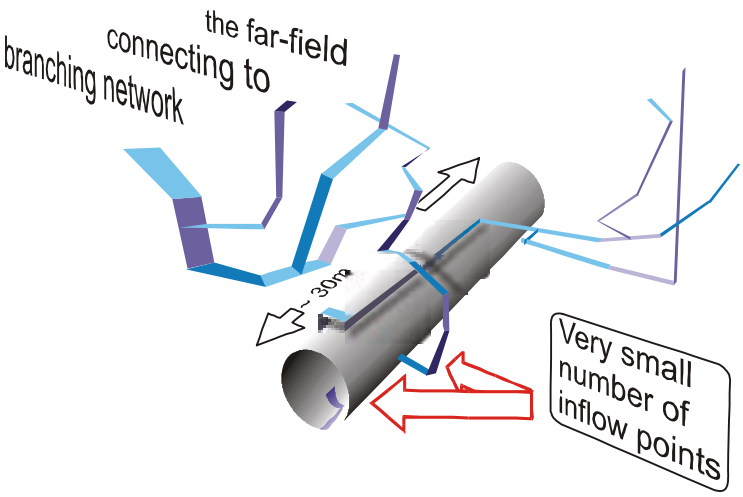

Figure 3. *Schematic illustrating the nature of how a sparse channel network probably interacts with a drift.*

Contents

1 Introduction

1.1 What underground experiments reveal about the region immediately behind the drift surface, the Excavation Damaged Zone (EDZ)

The near-field region, that is the rock within a drift diameter of the drift surface, contains the Excavation Damaged Zone (EDZ). It is conceived by rock mechanicists as a region of enhanced fracture opening and hence increased hydraulic conductivity and by hydrogeologists as a skin of reduced conductivity. It is useful to take a broad view of experimental experience in order to deduce an explanation for these apparently contradictory views.

The most frustrating experiments in underground research laboratories (URLs) have been tracer experiments and, the nearer they have been placed to drifts, the less predictable has been the tracer recovery. It would seem self-evident that hydraulic gradients close to drifts containing atmospheric pressure are very large and obviously orientated towards the nearest drift. However, the results of the so-called '3D migration experiment' at Stripa /Birgersson et al. 1994/ showed two significant aspects of the near-field. Firstly, when water flows into an unlined drift in fractured rock, very few of the fractures evident on the drift surface participate in the process: the bulk of the drift surface is dry. Secondly, tracers, injected only a few metres into the near-field, do not discharge into the drift at the nearest point and sometimes migrate many tens of metres in a direction seemingly unrelated to the apparently obvious head gradient.

Both pieces of evidence point to flow in the near field occurring in very discrete channels often orientated sub-parallel to the axis of the drift rather than radially. Virtually all hydraulic models of flow towards drifts conceive flow as converging radially with cylindrical symmetry. This assumes that all flow is perpendicular to the axis of a drift. Hence evidence and interpretation model disagree.

We have therefore developed the idea that the region of apparently reduced hydraulic conductivity is actually a region of extra head loss due to 'flow convergence'. It is extra to the normal convergence involved in radial flow to a line source (often termed 'cylindrical flow') in that it occurs parallel to the axis of a drift or borehole (see Figure 1-1). We have coined the term 'hyper-convergent flow'. It is analogous to partial penetration in porous medium aquifer well testing.

In order for it to occur, there has to be a limited number of inflow points to a drift or borehole that 'gather' flow from a larger number of flow 'features' (fractures or channels). This also means that the network of flow features making up the natural flow system must be sparse.

This report summarises a brief investigation into the concept of hyper-convergence.

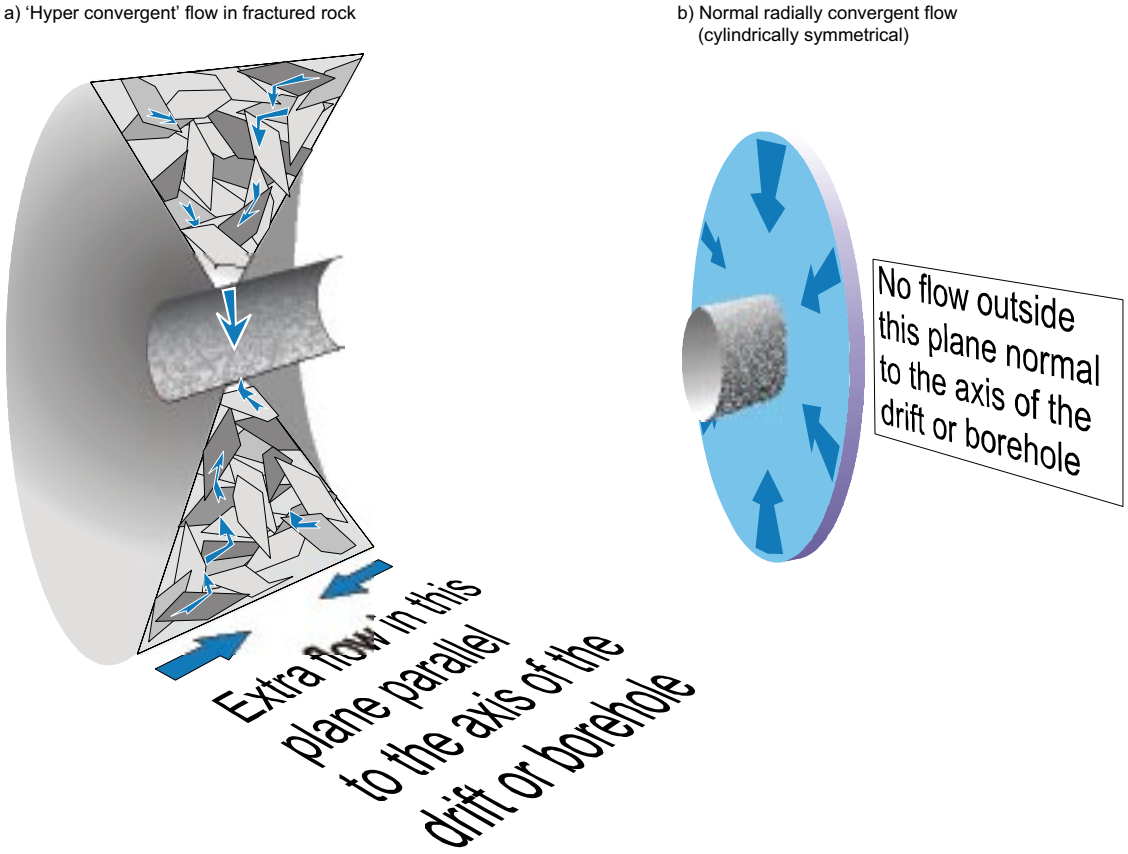

Figure 1-1. *The concept of hyper-convergent flow towards a drift or borehole.*

1.2 Scope of this report

The concept of hyper-convergence emerged from a review of experience in URLs concerning excavation damage /Black and Barker 2002/. Hence, this report begins by summarising some of the key experiments that provide insights into flow behaviour in the near-vicinity of drifts in fractured crystalline rock. This is preceded by a short section on the analysis of inflows to drifts. The next section of the report concerns the construction and use of an innovative channel network model designed to simulate flow behaviour in sparse networks of channels. A brief set of initial results is presented. They are then analysed to gain insights into how flow occurs in a sparse network and how apparent skin effect and derived hydraulic conductivity are related to each other and to the parameters used to create the network. Additionally they are discussed in relation to real experimental data from Stripa Mine. Next the report attempts to outline the wider implications of the concept of sparse channel networks if it applies widely. As is inevitable in a pilot study of this kind, many more questions have been raised than could be tackled in this project. Some of these ideas are briefly outlined in Appendix C.

2 Analysis of groundwater inflows to drifts/tunnels

This section is not intended to be either profoundly theoretical or comprehensive. It is included here in order to help understand the ideas presented later and the particular form of graphical outputs that are used.

Mathematical analysis of inflows to tunnels is limited, mainly because most important applications concern heterogeneous rocks under transient conditions. However, an exact analytical solution has been developed by /Lei 1999/, for steady-state inflow to a horizontal tunnel below the water table in a homogeneous, isotropic, semi-infinite, porous medium (Figure 2-1a).

Using the notation shown in Figure 2-1b Lei derived an equation for flow rate (q) into each linear metre of tunnel. Hence:

$$= \frac{2\pi K(d + p_a - \phi_0)}{\ln[D/r_t + \sqrt{(D/r_t)^2 - 1}]} \qquad (2.1)$$

where K is the hydraulic conductivity of the homogeneous, isotropic porous medium

and $\varphi_0 = p_a - D$.

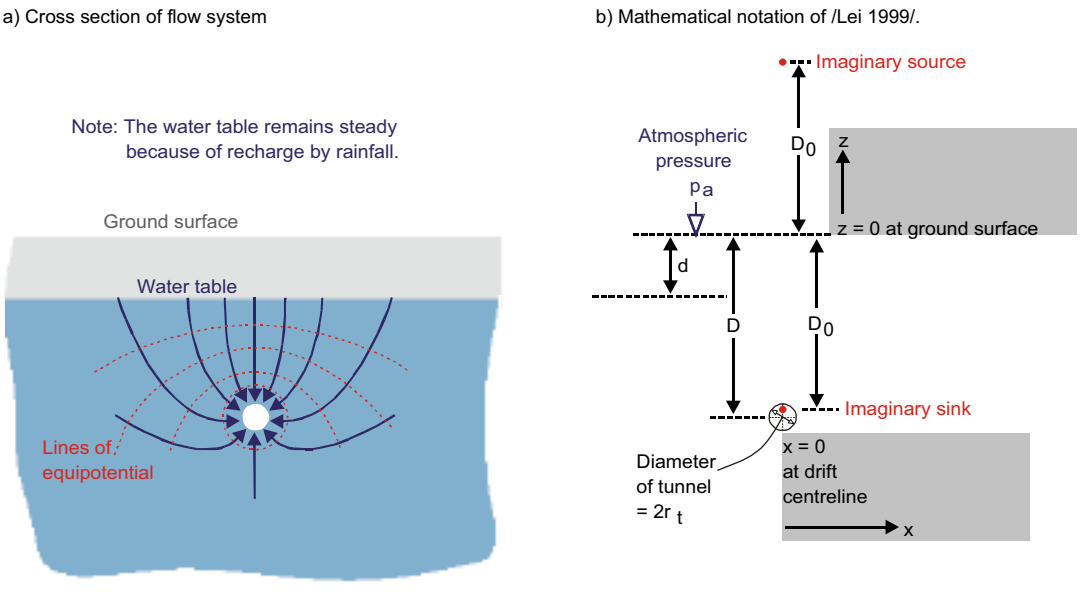

Note: A drift is a blind-ended tunnel.

Figure 2-1. *Schematic to illustrate the concept of 'steady-state' inflow of groundwater into a tunnel. a) flow concept. b) mathematical notation of /Lei 1999/.*

He also derived an equation for hydraulic head everywhere in the system:

$$\phi = \frac{d + p_a - \phi_0}{2\ln\left[D/r_t + \sqrt{\left(D/r_t\right)^2 - 1}\right]} \ln\left[\frac{x^2 + (z + D_0)^2}{x^2 + (z - D_0)^2}\right] + d + p_a \qquad (2.2)$$

where $D_0 = \sqrt{(D^2 - r_t^2)}$. (2.3)

It is apparent from Figure 2-1a that although the system is symmetrical about the 'z' axis it is not symmetrical about the centre-line of the tunnel and the head gradient from above is steeper than that from below. This asymmetry diminishes with increasing depth of the tunnel below the water table and is illustrated in Figures 2-2a and 2-2b. Both figures show hydraulic head versus distance from the centre-line of the tunnel in 3 different directions: vertically upwards, horizontally and vertically downwards.

Effectively, if the tunnel is located sufficiently far below the water table, then it will induce virtually symmetrical cylindrical radially convergent flow in the vicinity of the tunnel, as evident in Figure 2-2b. The effect of making 'D' very large in Equation 2.1 means that it reduces to:

$$q = \frac{2\pi K(d + p_a - \phi_0)}{\ln\left[2D/r_t\right]} \qquad (2.4)$$

In 1965, /Goodman et al. 1965/ derived a version of Equation 2.4 that can be considered a special case of the scenario shown in Figure 2-1. They conceived the water table as being located below ground surface and denoted the distance between the tunnel centreline and the water table as 'H_0' (or 'd = 0' and 'D = H_0). Assuming that the head everywhere at the tunnel perimeter is equal to the hydraulic head at ($x = \pm r_t$, $z = -H_0$), i.e. $\phi_0 = -H_0$, Equation 2.4 becomes the widely known 'Goodman formula' for general tunnel inflow. Hence:

$$q = \frac{2\pi K H_0}{2.3\log_{10}\left[2H_0/r_t\right]} \qquad (2.4a)$$

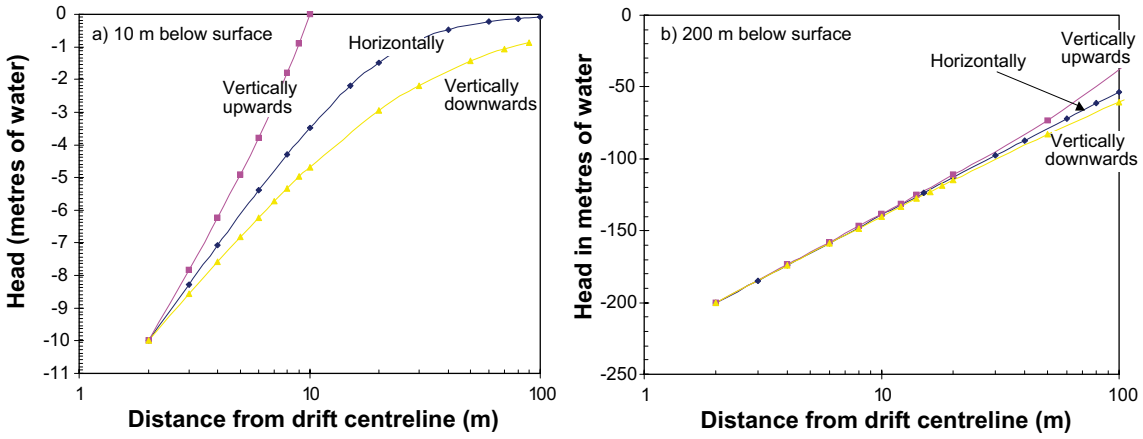

Figure 2-2. *The variation of head with distance from the centre-line of a 4 m diameter tunnel located; a) 10 m below the surface and b) 200 m below the surface. (The water table has been set coincident with the surface in both cases. The tunnel perimeter is set at atmospheric pressure.)*

Using Equation 2.4a, the only information needed to calculate inflow to a tunnel is the depth below the water table, the dimensions of the tunnel and the overall rock hydraulic conductivity. Using measurements of inflow, the Goodman formula is commonly used to derive a value for rock hydraulic conductivity. Alternatively, a more region-specific value of hydraulic conductivity can be derived from observations of head. For a typical tunnel, this is accomplished by plotting head, measured in nearby boreholes, versus the logarithm of the distance of the measurement point from the centreline of the tunnel (Figure 2-3a) and then using the slope of the best-fit straight line, Δs, in a modified version of the 'Goodman' equation. Thus:

$$K = \frac{2.3q}{\pi \Delta s} \tag{2.5}$$

where q is the inflow to the tunnel per unit length of tunnel,

and Δs is the drawdown per log cycle (to the base 10) (as shown in Figure 2-3b).

As stated earlier, this theory is founded very strongly in the porous medium concept. In the homogeneous, isotropic, porous medium theory, the measurements shown in Figure 2-3a would all lie directly along a straight line. In the reality of fractured rocks, it is assumed that the observed heads will not fit 'neatly' along a perfect straight line. Hence it is reasonably intuitive to assume that, the more the observations are displaced away from the 'best-fit' straight line (as in Figure 2-3c), the more heterogeneous is the rock in terms of hydraulic conductivity.

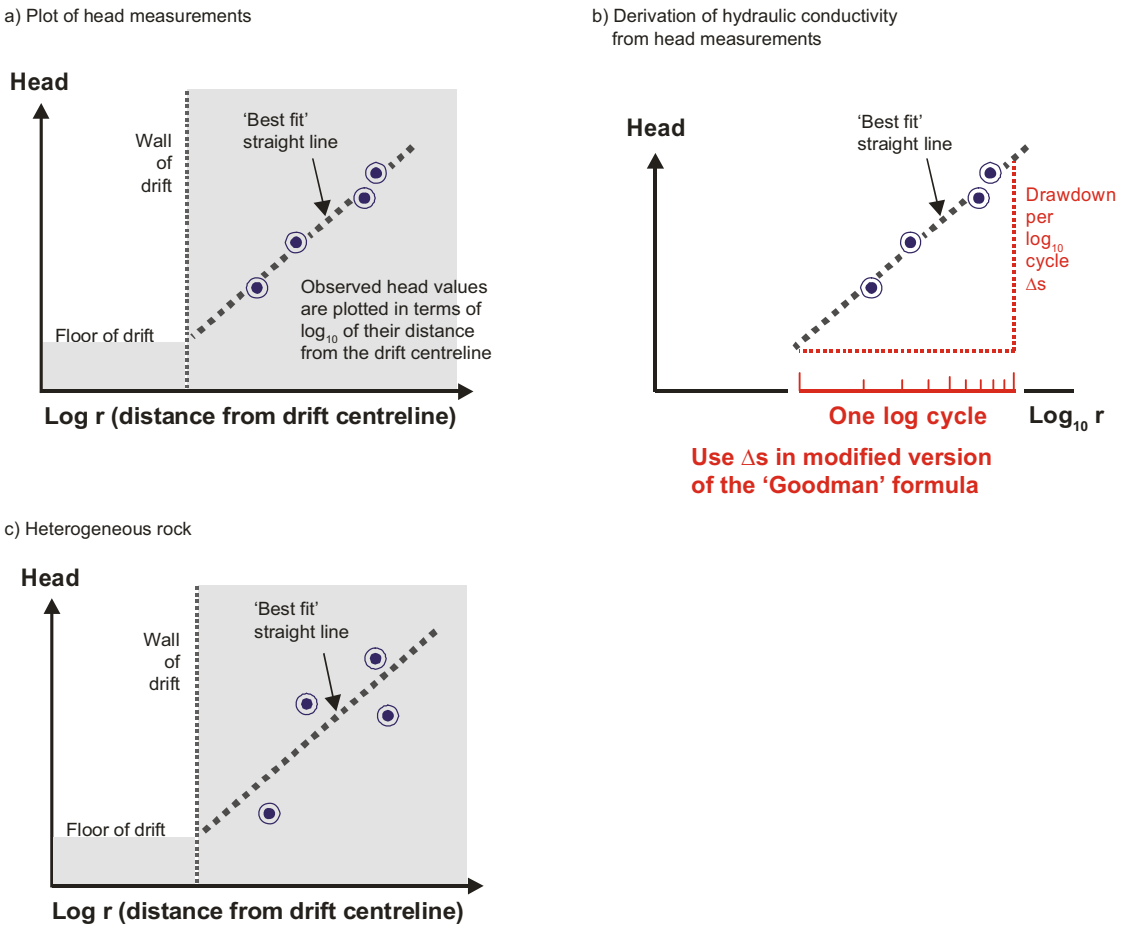

Figure 2-3. *The use of head measurements in the vicinity of a tunnel to derive a value for hydraulic conductivity that applies to the porous medium around the tunnel.*

It is common in tunnelling and mining to assume that the hydraulic conductivity of the rock immediately around an underground opening is altered by the excavation process (i.e. blasting, stress relief, air ingress, etc.). This immediate zone of altered properties is known in repository design as the 'Excavation Damage Zone' (EDZ). It has become commonplace to borrow a concept from groundwater hydraulics to describe it quantitatively, that of 'skin'.

In groundwater hydraulics, the skin effect is defined as the difference between the total drawdown observed in a pumped borehole and that resulting only from aquifer head losses. It is often assumed, as it is here in poorly transmissive rocks, that non-linear well losses (effects such as turbulence for example) are negligible. Adding the skin effect to the Goodman formula yields,

$$H_0 = \frac{q}{2\pi K}\left(\log_e\left[2H_0 \big/ r_t\right] + SF\right) \tag{2.6}$$

where q is steady state inflow per metre of tunnel

SF is dimensionless "skin factor"

H_0 is the depth of the tunnel centreline beneath the water table

and $SF\ q/2\pi K$ is "skin effect" in metres (of head of water). (2.7)

Because the concept is borrowed from groundwater hydraulics, drawdown is measured as a positive quantity and "skin factor" is positive when the skin effect 'adds' to the observed drawdown. Skin effect is observed in the vicinity of drifts by using the same 'log r' plot of heads as is used to determine the overall rock hydraulic conductivity (see Figure 2-3 above). Unlike the situation around boreholes where the physical configuration renders identification of the thickness of the skin zone impossible, it is comparatively straightforward around drifts.

Using 'log r' plots, several outcomes are possible. In the first case (Figure 2-4a), point measurements of head in boreholes around a drift are plotted versus the logarithm of distance from the drift centreline. If there is cylindrically convergent flow and homogeneous properties right up to the drift wall, there should be no skin effect and the best-fit straight line through the measurements should intersect the borehole wall at the floor level (Figure 2-4a). If the rock in the immediate vicinity of the drift is damaged by excavation such that a 'skin zone' of reduced hydraulic conductivity occurs (Figure 2-4b), then the best-fit straight line through measurements from beyond the 'skin zone' will, when extrapolated, intersect the drift wall at a value equal to the "skin effect" (i.e. Equation 2.7). In reality, the thickness of the 'skin zone' is unknown and measurements within the 'skin zone' would reveal an increased apparent gradient (as in the inset to Figure 2-4b). The situation is reversed where excavation damage produces a 'skin zone' of enhanced hydraulic conductivity (see Figure 2-4c) and the value of "skin effect" becomes negative. Generally speaking however, measurements within the 'skin zone' are virtually unheard of.

Skin is sometimes viewed in terms of an 'effective radius' in that a borehole or drift with positive skin appears smaller, when distant drawdown measurements are plotted versus 'log r', than its actual physical dimension. In groundwater hydraulics, effective borehole radius (r_{eff}) is related to actual borehole diameter ($2r_{bh}$) by the equation:

$$r_{eff} = r_{bh}e^{-SF} \tag{2.8}$$

The same relationship applies here to drifts and its derivation from 'log r' plots is shown in Figure 2-4.

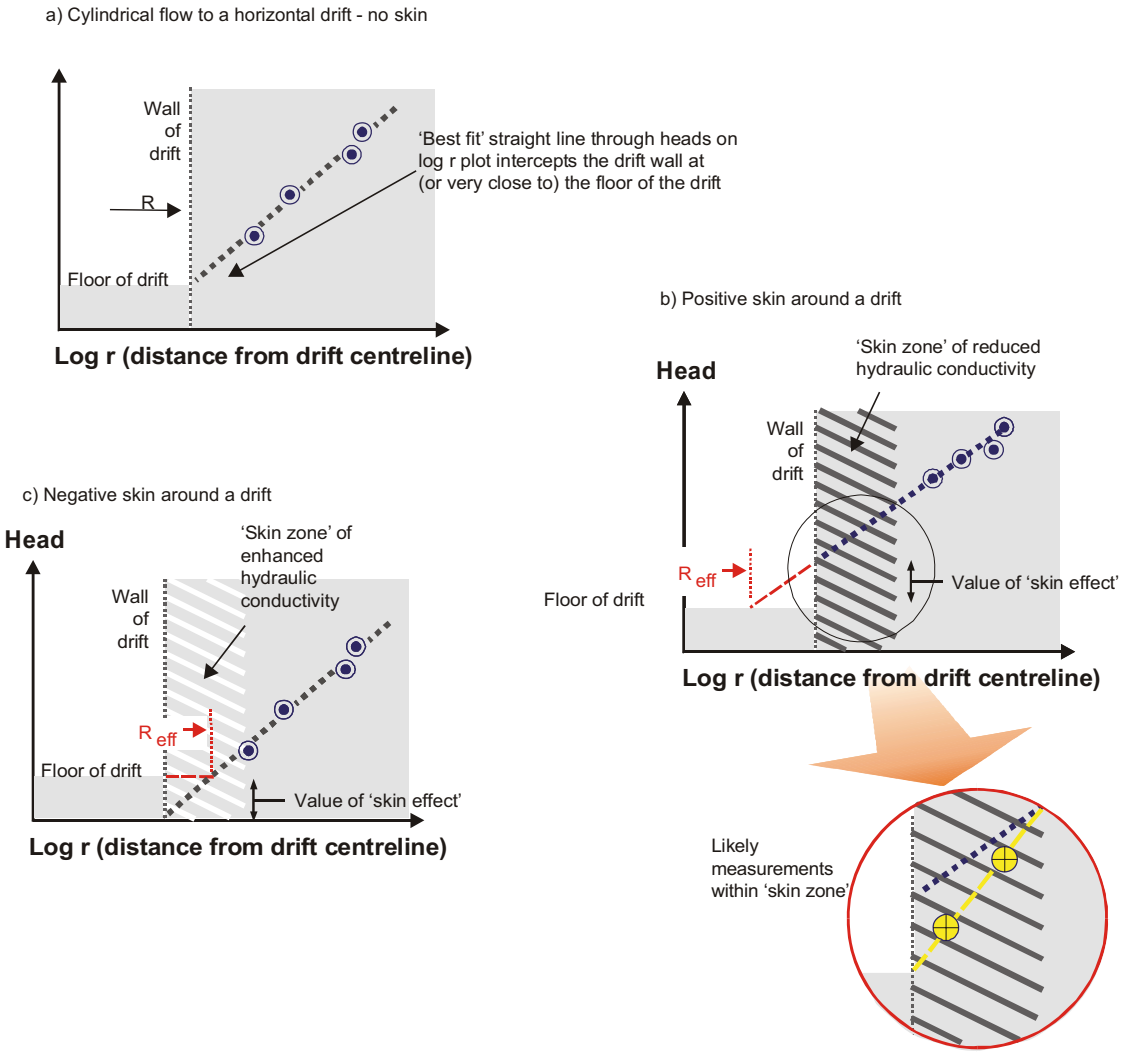

Figure 2-4. *Using head versus distance results to derive the hydraulic conductivity and value of 'skin' for the rock around an open drift.*

3 Hydraulic measurements of the EDZ at Stripa

This brief review concerns hydraulic measurements of the region in the immediate vicinity of the drift wall in the Stripa Mine. It is not comprehensive but is intended to highlight the evidence for groundwater flow in sparse networks.

The Stripa Mine was an abandoned iron ore mine in central Sweden where some new drifts were excavated to perform underground experiments. Experiments were designed and performed by various consortia of investigative organisations in three phases over a period of 15 years.

3.1 The 'large-scale Macro-Permeability' experiment (1977–1981)

The 'Macro-Permeability' experiment was designed to assess how to 'scale up' small-scale borehole measurements of fracture transmissivity to predict large-scale hydraulic conductivity ('macro-permeability'). A major aspect of the experiment was the use of the difference in moisture content between incoming and outgoing ventilation air from a sealed-off drift to measure overall inflow.

The experiment involved measuring the groundwater inflow to a 33 m long drift whilst also measuring groundwater pressure in 64 packer-isolated intervals in 10 boreholes installed from the drift in the radial pattern shown in Figure 3-1a. According to /Gale et al. 1982/, *"Each interval was about 5 m long; a length intended to include sufficient numbers of fractures (generally 15 to 20) within each zone to provide reasonable assurance that the pressure data would be sufficiently averaged to produce smooth pressure profiles".* In the event, this did not prove to be the case (Figures 3-1b and 3-1c). Although some boreholes, R3, R4, R6 and R9, exhibit consistent head declines towards the drift, the rest show sudden drops and peaks. The values shown in Figures 3-1b and 3-1c are all derived from a paper by /Witherspoon et al. 1981/ and the division into 'floor' and 'roof' categories is a new representation. In the original paper, 5 packed-off zones were depicted as having a head equal to the floor of the drift. It was not clear whether this was a packer malfunction, a real value or an air-filled zone so all 5 zones were ignored in the derivation of 'average' gradients. Although it may appear otherwise, the 'roof' series has less scatter than the floor series (an 'R^2 value' of 0.35 compared to 0.24). The $\log_{10}$ slope of the 'roof' series (Δs) is 68.6 m compared to 35.1 m for the 'floor' series. Unfortunately, the ventilation method of water abstraction means that the distribution of inflow between floor, walls and roof is unknown but, if it were evenly distributed, then the 'floor' would be roughly twice as conductive as the 'roof'. However, it should be borne in mind how the air-water interface adjusts following excavation in that it recedes into the roof of the drift leaving a sort of 'spring line' along the walls about a third of the way up (Figure 3-2b). Hence the 'roof' boreholes (Figure 3-1b) should have an unsaturated region where they intercept the drift whereas the 'floor' boreholes (Figure 3-1c) should all intersect the drift below the 'spring line'. It is relatively surprising that both sets of boreholes appear to have a 'skin effect' of equal magnitude, about 45–50 m.

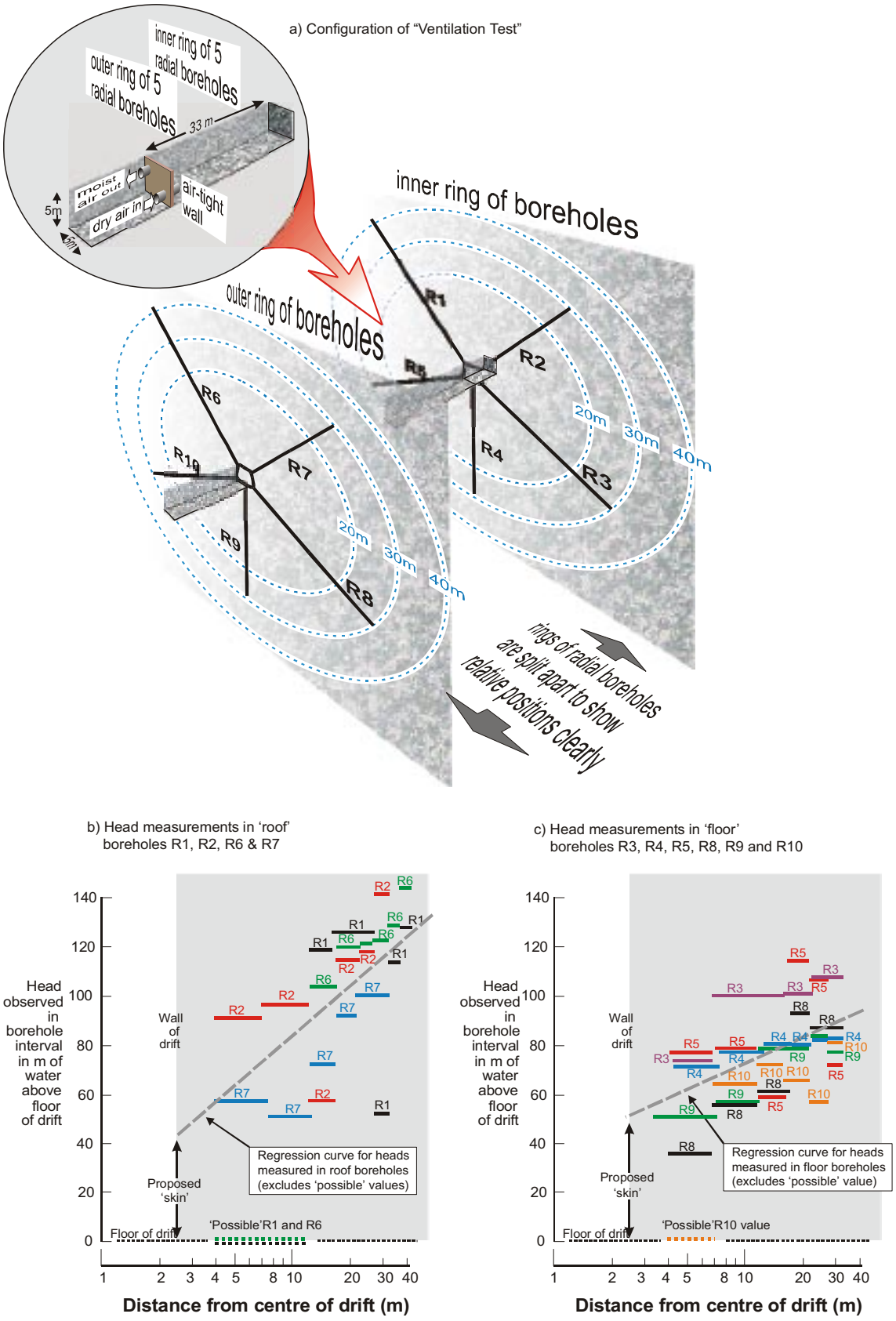

Figure 3-1. *Schematic summary of the 'Macro-Permeability experiment' based on /Gale et al. 1982/. a) General layout of the experimental drift with 2 'rings' of 5 radial boreholes. A splay of 5 boreholes emanating from the end wall are not shown. b) and c) Summary of the head measurements performed in the radial boreholes (lines are best-fit regression lines).*

The hydraulic conductivity of the rock surrounding the 'Macro-Permeability experiment' was evaluated using 2 different methods. The first was to measure the total inflow of groundwater into the drift and then assume that the 'Goodman formula' (Equation 2.5) could be applied (Figure 2-3). This requires the evaluation of the average Δs for the entire radial head dataset excluding the 5 zero values (Figure 3-3a).

/Gale et al. 1982/ derived a value of *"about 1.0×10^{-10} m/s"* for the *"average rock mass permeability"* which is roughly half the value derived here as indicated in Figure 3-3a. This is because the /Gale et al. 1982/ paper shows only a limited set of head data and so Figure 3-3a is based on a full dataset from /Witherspoon et al. 1981/. It is not entirely clear how /Gale et al. 1982/, calculated their value of permeability but they use terms such as 'weighted average' and 'simplified analysis', derive a different best-fit slope and have unlikely high values of 'correlation coefficient'. Regardless of the causes, the difference is only between 1×10^{-10} and 2×10^{-10} m/sec.

The second method was to take an average of packer test results (Figure 3-3b) conducted in all 15 boreholes originating in the drift (i.e. 10 radial and 5 end wall). The analysis of each test assumed that the test interval was a homogeneous porous medium. /Gale et al. 1982/ assumed also that there was no overriding geometric configuration to the hydrogeological system and therefore proposed the geometric mean of the distribution as the putative large-scale value.

The use of the 'log R' plot also led /Gale et al. 1982/, to speculate about the thickness and nature of the skin. They decided that if the 'skin' is 2.5 m thick (i.e. half a drift diameter) then its hydraulic conductivity would be ~ 7×10^{-11} m s^{-1} or about one third of the average large-scale value (Figure 3-3a). It should be noted that there were no direct observations conducted within this putative skin zone.

The Macro-Permeability experiment threw up several interesting questions. When they tried to increase the effective pumping rate by increasing the evaporation rate, the measured inflow to the drift declined. A possible explanation is that the air-water interface moved deeper into the rock and that the average length of a flowpath to an inflow point increased.

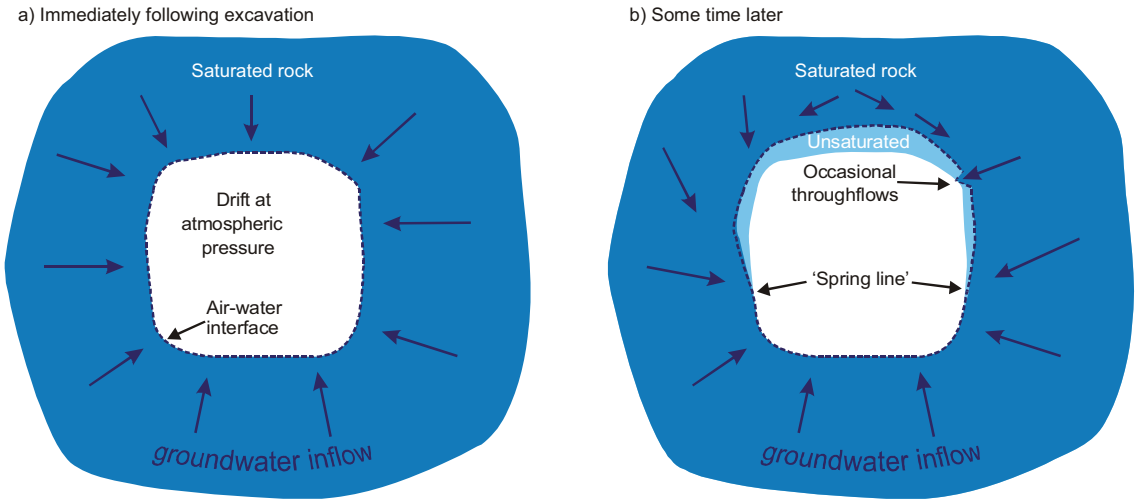

Figure 3-2. *Schematic cross-section of a drift illustrating how the air-water interface around a drift migrates after excavation.*

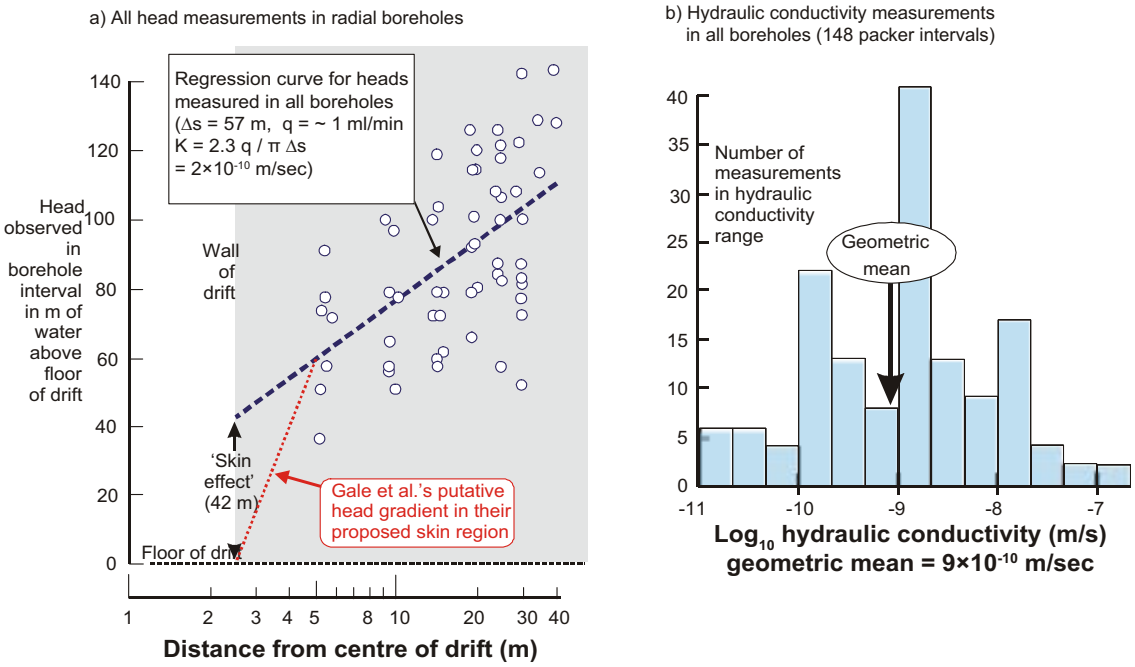

Figure 3-3. *Two methods to evaluate hydraulic conductivity in the vicinity of the Macro-Permeability experiment: a) heads measured around the drift plotted as 'mid-point' values. b) packer test results in the boreholes around the drift (test interval lengths vary between 2 and 4 m.*

/Rouleau and Gale 1982/ spent a lot of time measuring fractures in underground openings and borehole cores and decided there were 4 fracture sets present with mean spacings of 0.93 m, 0.36 m, 0.79 m and 0.51 m. They estimated tracelengths and because of not being able to observe both ends of fracture traces ended up with values ranging between 1 and 6 m, most observations obviously were only a little above 1 m. Hence, the rock of the Macro-Permeability experiment was portrayed as well fractured on a 1-metre scale, which is seemingly at odds with the variability exhibited in Figure 3-1.

3.2 The 'Simulated Drift Experiment' (1988–1992)

The 'Simulated Drift Experiment' was part of a larger experiment to assess how well numerical models could predict flows in fractured rock. Essentially, five 100 m long boreholes were drilled from an experimental drift in a cylindrical pattern (Figure 3-4a) around a central borehole into a region of reasonably well-characterised rock containing a number of fracture zones /Olsson 1992/. The boreholes were then allowed to discharge at three fixed head steps and the discharge measured. In this way they 'simulated' a drift. The next step was to excavate an actual drift (known as the 'Validation Drift') for a distance of 50 m using the 5 boreholes to define its circumference, and leaving a further 50 m of the pre-existing boreholes in place (Figure 3-4b). The ceiling and upper walls of the Validation Drift were covered in segmented flexible plastic sheets designed to collect all groundwater discharge from rectangular areas of 2 m^2. The floor and lower walls were also configured into rectangular areas and inflows collected in sumps and measured. Since the floor was mostly open to the mine ventilation the whole drift was isolated with an airtight bulkhead (similar to the 'Ventilation test' above) to ensure no inflow was unaccounted for. Apart from some very short boreholes drilled into the floor to act as collection sumps, there were no boreholes drilled from the Validation Drift.

The major result from the comparison between the Simulated Drift and Validation Drift inflows was the significant reduction in inflow to the excavated drift (Figure 3-4c). After taking account of the features intersected by the first 50 m of the boreholes, inflow to the Validation Drift was just 12% of the value for the combined total of equivalent sections of all 6 boreholes. This was a reduction by a factor of 8.

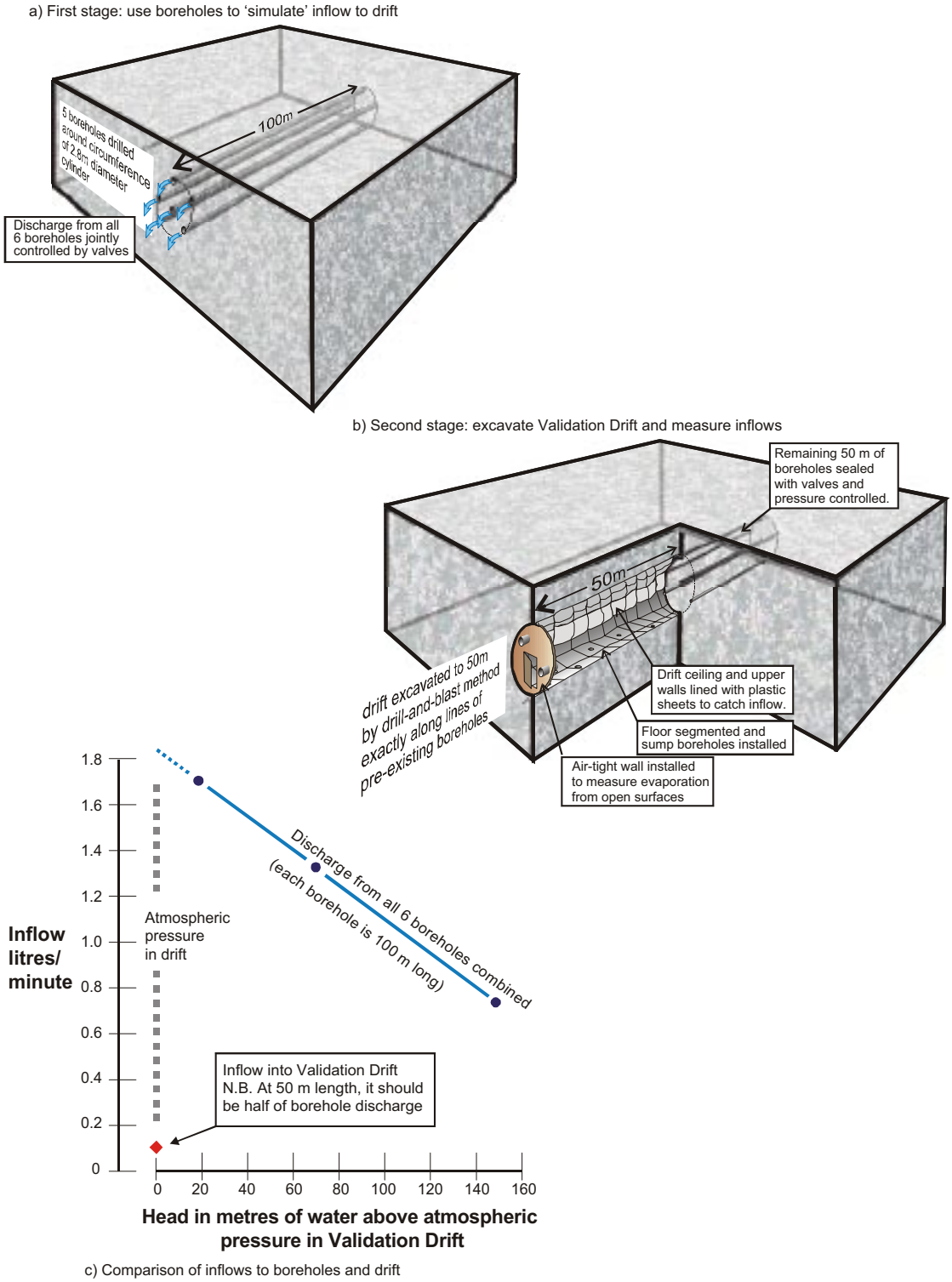

Figure 3-4. *Basic hydrogeological components of the Site Characterization and Validation Project showing a) the Simulated Drift Experiment b) measurement of inflows to the Validation Drift, and c) combined inflow results showing large reduction in inflow to the Validation Drift.*

There was a secondary set of observations from the Simulated and Validation Drift experiments that gained much less prominence at the time but which was probably equally important in understanding the processes that were producing the results. (The reasoning and the observations underpinning the conclusions below are described in more detail in Appendix A.) They are:

- Flows to the 6 boreholes of the Simulated Drift showed that, at least, some of the flow features were independent of each other at the scale of 2 m. In other words, at least some of the flow features were channels that could 'fit' between adjacent boreholes of the Simulated Drift. This implied a channel width of less than 2 m.
- Flows to both the Simulated Drift boreholes and the Validation Drift were very localised so that a few features accounted for the vast majority of the inflow in both configurations. There were about 6 inflow areas in 50 m length of Validation Drift and about 20 in the 6 Simulated Drift boreholes with the same overall length dimension. The 50 m of drift had an internal surface area of about 440 m^2 of which approximately 62 m^2 was described as 'wet rock', or 14% of the surface area. About 50% of the inflow came in one small area.
- Only the Validation Drift experiment unambiguously exhibited a 'skin zone' of reduced hydraulic conductivity (~ +120 m) albeit based on extrapolating rather distant head measurements back to the drift wall. The borehole array, the Simulated Drift, gave ambiguous results in that when heads were extrapolated back to the centre the most likely interpretation was that the 5 circumferential boreholes appeared to give the central borehole a negative (rather than positive; i.e. enhanced conductivity) skin (~ –20 m).
- The Validation Drift yielded a value of 'large-scale' hydraulic conductivity of ~ 3 E–10 m s^{-1}. The equivalent value for the Simulated Drift was ~ 2E–9 m s^{-1}. Since the large scale hydraulic conductivity was not altered by the excavation of the Validation Drift this is a surprising result. The Validation Drift value is very similar to that obtained from the earlier 'Macro-Permeability' experiment.
- When the Simulated Drift was converted to the Validation Drift, the 'skin' was observed to develop gradually over a period of days after initial excavation.

3.3 Summary of Stripa hydraulic experiments

In conclusion, the experiments at Stripa showed relatively consistent behaviour. Flow appeared to be localised in channels so that even 'whole-drift' experiments, such as the Macro-Permeability test, did not produce homogeneous head fields. The channels appeared to be relatively sparse in the sense that 50 m of open drift contained a 'handful' of inflow points with few extending outside one or two 'catchment sheets' (with an area of 2 m^2). Both open-drift inflow experiments appeared to be associated with the development of a positive skin of considerable magnitude. The Simulated Drift experiment probably did not contain a skin. Instead the configuration may have resembled hydraulically a single central borehole with negative skin.

It was decided that the Simulated/Validation Drift experiments were more complex than the Macro-Permeability test. Since the simpler test exhibited an apparent skin, thought to be explicable with the concept of hyper-convergence, the modelling reported below aimed to imitate the Macro-Permeability test as a first step. Nevertheless, the observations from the other experiments were borne in mind in the formulation of the modelling.

4 Numerical modelling using a sparse channel network

4.1 Introduction

The key to the concept of hyper-convergence is that flow into a drift has to be limited to a few points and that flow must be forced to converge to those points via connections with the wider network of flow features. In other words, network sparseness is critical to the behaviour. Based on the review of experience at Stripa, a channel, rather than a fracture, network was chosen as the preferred modelling approach. This was in response to the 'patches' of inflow observed in the Validation Drift (Figure A1-4) and the persistent flow from the central borehole of the Simulated Drift (Figure A1-1).

This section describes how a channel network model has been developed from scratch and gives some initial results relevant to assessing the validity of the concept of hyper-convergence.

4.2 Basic approach

The idea is to set up a numerical model of a region of fractured rock, to calculate flows into a tunnel and to derive the skin effect and conductivity parameters in a similar way to that used in the field.

The model described here is based on individual flow channels. As a modelling convenience, these are constrained to sit on a lattice. The interconnectedness of the lattice channels can be varied by altering the way they are generated. The lattice is assumed to be statistically homogeneous – no attempt is made to include known features. The assignment of all lattice characteristics (location of channels and their properties) is stochastic.

4.3 Lattice construction

The channels are constructed on a 3D cuboidal lattice. The lattice size and spacing can be chosen to suit the situation being modelled. At this preliminary stage, spacing is the same in each direction, but it is recognised that increased spacing in one or two directions (causing anisotropy) might be useful in subsequent studies. The lattice nodal positions could be perturbed in other ways to give a less rectangular effect but this is also not included in the current study.

The network is formed by creating bonds between the nodes of the lattice. Only a fraction of the total potential bonds (node to neighbouring node connections) are present in the model system. A channel is conceived as a set of bonds in a continuous row. Bonds could be created at random, but this would create a lot of unrealistic short channels. Longer channels are thought to be more realistic, and so some correlation between sequential bonds is required. To achieve this, two parameters are used to characterise the system. Both are probabilities:

P_{new} is the probability of starting a new channel if the previous bond was absent;

P_{again} is the probability of continuing a channel to a subsequent bond.

From these, the probability, P_{on}, that a bond is present can be deduced. By considering the probability that a bond is present given the state of the previous bond:

$$P_{on} = P_{on}P_{again} + (1 - P_{on})P_{new}, \tag{4.1}$$

which gives

$$P_{on} = \frac{P_{new}}{1 - P_{again} + P_{new}} \tag{4.2}$$

Also, the average number of bonds of a channel can be seen to be

$$B_{ave} = \frac{1}{1 - P_{again}} \tag{4.3}$$

In practice then, each line of bonds is considered in turn. The first bond has probability P_{on} of being present and then the P_{new} and P_{again} probabilities are used for each bond in turn.

Two approaches to assigning hydraulic properties can be used. Either the whole of a channel is assigned the same value, or each bond is assigned a value separately. The former approach has been used in the calculations presented later. In either case, the property to be assigned is a conductivity times area (or transmissivity times width). Equivalently this is a conductance per unit length and so is referred to here as a specific conductance, and is denoted as C_S. A central value, $\overline{C_S}$, is set and a log-normal distribution of values is created with a specified standard deviation (for the $\log_{10}$ value).

To relate the C_S to an overall conductivity we argue as follows:

The average C_S per lattice node is equal to the central C_S times the probability of a bond being present divided by the relevant area, and this corresponds to the overall conductivity, $k_{creationl}$, so (assuming that the lattice spacing is S in all directions)

$$k_{creation} = \frac{P_{on}\overline{C_S}}{S^2} \tag{4.4}$$

Whilst this approach is appropriate for a reasonably well-connected system, it can only be expected to give a very approximate value for poorly connected systems. It can be inverted to give a suitable $\overline{C_S}$ from the overall conductivity. The effect of altering the choice of bond creation probability, P_{new}, is illustrated in Figure 4-1.

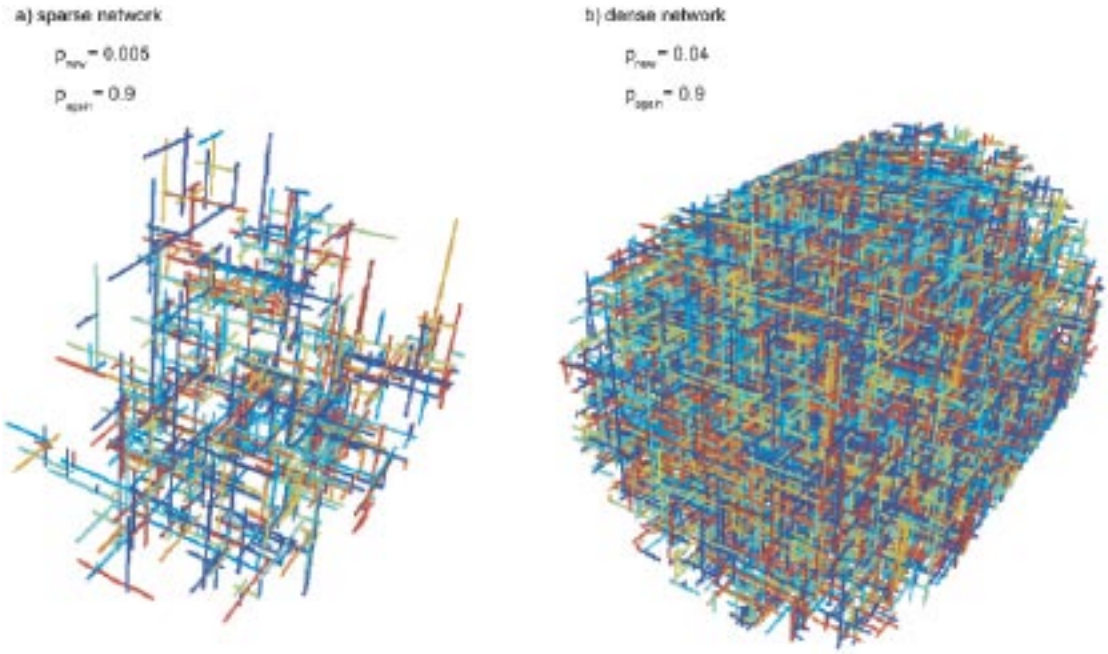

Figure 4-1. *Examples of sparse and dense channel networks.*

4.4 Flow system

Two different flow systems are solved. The first is the full cuboidal region without any tunnel. The top and bottom boundaries are given different heads and a vertical flow is calculated. This provides a measure of the large-scale hydraulic conductivity and is termed the ‘face-to-face K’.

The second flow system to be solved consists of a cylindrical tunnel extending the full extent of one direction (taken to be x) with a cylindrical outer boundary at a specified distance from the tunnel centreline. The boundary conditions on the x boundaries are no flow (i.e. symmetry). The outer boundary has a fixed head and the inner tunnel wall is also at a specified fixed head (taken to be zero). Note that strictly the tunnel should be at a fixed pressure (atmospheric) and the head should vary slightly around it, but for a small tunnel this is insignificant (and would introduce requirements to ensure that flow did not emerge from the tunnel). This flow solution also provides a measure of system hydraulic conductivity that is here termed the ‘line sink K’.

Prior to solving either flow system, any nodes that are not connected through the flow system are removed from consideration. In the first case, this means any node not connected to both the top and bottom faces. In the cylindrical flow configuration, nodes not connected to both the tunnel and the outer boundary are removed. It is essential to find completely isolated nodes in order to avoid singular matrices. The others are removed to reduce the problem size since they would have head equal to either the tunnel or the outer boundary and would be stagnant (see Figure 4-2).

The remaining network has mass conservation applied at each node with a linear, Darcy, relationship between flow and head difference in each bond. The resulting linear equations for the head can be solved using standard numerical methods. They are sparse and symmetric so a pre-conditioned conjugate gradient (PCCG) approach is favoured. For poorly

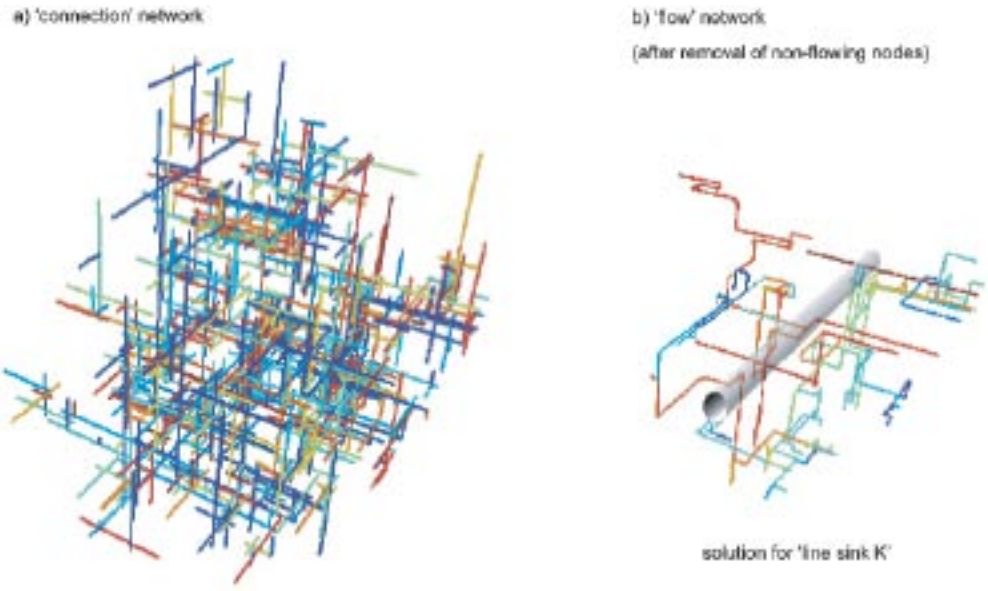

Figure 4-2. *Example of how the network is thinned out prior to solving the flow system.*

connected systems (less that 30% of the nodes active) a general purpose sparse matrix with a partial Cholesky pre-conditioner is used on a system containing only the active nodes. For fuller systems, the full lattice is solved using a specialised block-structured preconditioner.

4.5 Calculated outputs

The flow models can be used to calculate a number of outputs of which the following form the main results:

- The flows in each bond can be calculated from the calculated heads.
- For the vertical flow calculation, the total flow through the system is calculated and used to provide an average large-scale hydraulic conductivity, the face-to-face K.
- For the tunnel flow calculation a wider set of results is calculated.
- flows into the tunnel are reported by location, together with the total flow.
- The heads at each active node and the radial distance are reported and used to calculate the skin effect and (in conjunction with the tunnel flow), the implied conductivity, the 'line sink K'. This is based on using the Thiem equation common in porous medium hydrogeological reference texts. Its use in the context of the modelling reported here is described below.

Analytically, the head, in a homogeneous porous medium system containing a line sink abstraction such as a tunnel, is described by:

$$h = h_0 + (h_1 - h_0)\frac{\log(r/r_0)}{\log(r_1/r_0)}, \tag{4.5}$$

where the 0 and 1 subscripts refer to the tunnel and outer boundary respectively,

h refers to head,

and r refers to distance from the line source.

The flow to a tunnel (of length L) would be:

$$Q = 2\pi L r_0 k_{rock} \left.\frac{dh}{dr}\right|_{r=r_0} = 2\pi L k_{rock} \frac{(h_1 - h_0)}{\log(r_1 / r_0)}. \quad (4.6)$$

By substituting values for total calculated inflow into this equation and using the dimensions of the model together with its boundary condition head values, Equation 4.6 can be used directly to calculate K_{rock}. This is reported as 'simple fit'. It should be borne in mind that it is based on the assumption that flow converges radially to a line source and that there is no extra head loss due to a skin. It should also be borne in mind that the heads throughout the flow system and calculated by the model, take no part in the derivation of K_{rock} 'simple fit'.

An alternative, based on the change of head with distance from the line sink, uses the related expression:

$$h = h_0 + \frac{Q}{2\pi L K_{rock}} \log(r / r_0). \quad (4.7)$$

In the numerical model, a least-squares fit to the calculated head versus distance data is used to obtain:

$$h = h_{wall} + \alpha \log(r / r_0) \quad (4.8)$$

and derive K_{rock} 'head fit' from Q and α.

In general h_{wall} will not equal h_0 and this is what is meant by the skin effect. We write

$$h_{wall} = h_0 + h_{skin}. \quad (4.9)$$

Although the 'connected network' is thinned to produce the 'flow system network' by removing isolated nodes and those connected only to the inner or outer boundaries, there are still 'cul-de-sac' bonds within the system that contain no flow. These are distinguishable from nodes containing non-zero flows. Thus heads can be derived from 2 types of node. The least squares fitting is performed for all active nodes and then separately for nodes with non-zero flows, giving two estimates of K_{rock} and h_{skin} for 'all nodes' and 'flowing nodes'.

4.6 Software

The approach described is implemented in a Quintessa code, HyperConv. There is an associated viewer called LatticeViewer.dll that HyperConv can call. Both are described in more detail in Appendix B.

5 Modelling results

5.1 The dependence of calculated 'skin' on network generation parameters

Depending on the lattice properties chosen, it is possible to see cases with both positive and negative skin effects. There is a lot of variability in the results from realisation to realisation. Results are very sensitive to the P_{new} and P_{again} parameters.

The following use a 60×60×60 lattice and a 1.5 m separation (i.e. a 90 m cube), 2 m tunnel radius. All have 'whole-channel' conductivities with a $\log_{10}$ standard deviation of 2. In addition to the input probabilities, the table shows the calculated probability of any particular bond being active and the average length of channels.

Table 5-1. Preliminary values of skin (in metres of extra head loss) for a limited selection of network creation parameters (outer boundary = 200 m head, central drift = 0 m head).

P_{again}	P_{new}	P_{on}*	B_{ave}**	10 h_{skin} values (m)***					Average h_{skin} value (m)***
0.8	0.03	0.130	5	–11	9	14	0	–23	–15.9
				–27	–37	–36	–18	–30	
0.8	0.025	0.111	5	23	–6	–16	–44	–47	–18.7
				–20	–33	–23	–10	–11	
0.8	0.02	0.091	5	54	–67	–58	24	62	–5.5
				–64	–36	–10	30	10	
0.85	0.02	0.118	6.67	27	–4	20	4	–28	–1.4
				–12	5	33	–12	–47	
0.9	0.02	0.167	10	40	41	48	29	28	+22.8
				10	2	11	17	2	
0.9	0.015	0.130	10	58	33	27	1	27	+23.9
				12	30	9	26	16	
0.9	0.01	0.091	10	87	60	42	38	28	+40.4
				38	40	18	22	31	
0.9	0.005	0.048	10	50	58	46	24	92	+53.0
				71	39	44	18	88	

* P_{on} is the probability that a bond is present. i.e. P_{on} = 0.091 means 9.1% of all possible bonds are present. NB less than 9.1% will be connected and even less will contain active flow.
** B_{ave} is the average number of bonds of a channel.
*** Negative values of skin are highlighted in red.

Although Table 5-1 shows a limited number of preliminary values some trends are clear:

- For any single set of network creation parameters, the range of values of h_{skin} is large.
- Positive h_{skin} values are more likely in systems that have longer channels (P_{again} larger).
- Positive h_{skin} values are more likely in systems that have less connectivity (P_{new} smaller).
- The crude measure of network density, P_{on} , is not a predictor of h_{skin} (compare the first and sixth sets of results both with 13% active nodes and very different values of skin).

5.2 Organisation of heads and flows

The network properties appear from Table 5-1 to be highly variable even given the same generation parameters so it was of interest to examine the variability of the flows and heads (Figure 5-1). It is clear that a few paths take tunnel head values out to near the outer boundary and that much of the network is virtually unaffected by the flow system.

5.3 Quantitative investigation of head versus distance

The preliminary results above indicate that a positive skin of the same magnitude as that found in the field can be generated with a sparse network such as that in the bottom row of Table 5-1. These are the same generation parameters as were used for the illustrative results of Figure 5-1. It is already apparent that there is considerable variability from one network realisation to the next so the same generation parameters (i.e. $P_{new} = 0.005$, $P_{again} = 0.9$) were used to generate 100 realisations. Recall that this implies average channel lengths of 10 bonds (15 m in the rock), still a fraction of the total system size. It also has only 4.8% of the bonds being active.

The first of the 100 cases was run separately to obtain the full head output file. Figure 5-2 below shows the head versus log r plot for all the active nodes (even though many contain zero flow). The Excel trendline option is used to give the fit (this agrees with the value calculated by HyperConv). Removing the non-flowing nodes changes the derived values of hydraulic conductivity and skin together with the goodness of fit of the 'best-fit' straight line (Figure 5-3).

The reason for the changed values is comparatively straightforward. In general terms, the best fit line is more or less 'anchored' to the outer boundary of +200 m of head at 45 m radius. In the 'all nodes' version (Figure 5-2), the best-fit line is strongly influenced by a significant number of 'non-flowing' nodes that have high heads but extend to within a few metres of the inner (zero head) boundary. This reinforces the point noted on Figure 5-3b that there appear to be only 3 points of inflow into the drift. The high head nodes close to the drift far outnumber the 'non-flowing' low head nodes that extend towards the outer boundary, presumably because these are limited by having to be connected to the three active inflow points.

It should be borne in mind that:

K_{rock} = inflow / 2 π $\log_e$ slope

or K_{rock} = inflow / 2 π Δs

so that K_{rock} is inversely proportional to the slope in Figures 5-2 and 5-3b and the insets in Figure 5-4. This has a direct influence on the cumulative distribution functions for hydraulic conductivity derived from the 100 realisations shown in Figure 5-4. Several features of Figure 5-4 are noteworthy. Firstly, the values of 'face-to-face' K are significantly lower than all other values. Secondly, the remaining three determined values are all based on values of head and assuming that the head versus distance relationship conforms to cylindrically symmetric convergent flow to the imaginary drift. They are all similar in value but cover a much wider range than the 'face-to-face' value (3 orders of magnitude between the 10th and 90th percentile rather than two). Thirdly, the target hydraulic conductivity, $K_{creation}$ is

significantly larger than the median value of any of the CDFs. The largest difference is between the median value of the 'face-to-face' K distribution which is almost 100 times less. The origin of all the 'K' values and the relationships between the line-sink 'K' values are explained in the lower six diagrams on Figure 5-4.

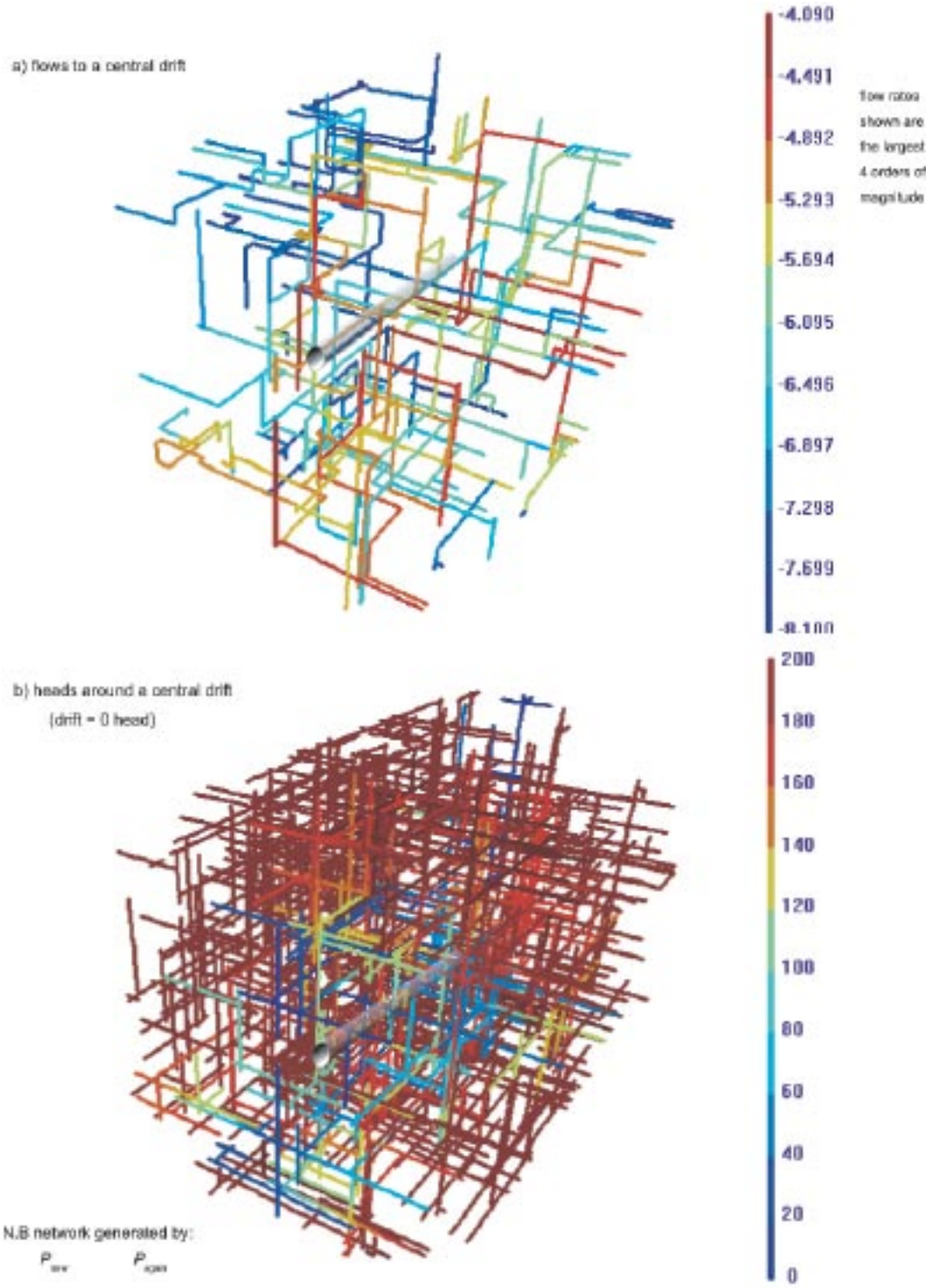

Figure 5-1. *An example of flow rates and heads around a central drift in a sparse network. The flow network appears much sparser because the majority of the active network has flow rates below the threshold for representation (i.e. less than 0.0001 of the maximum single channel flow rate).*

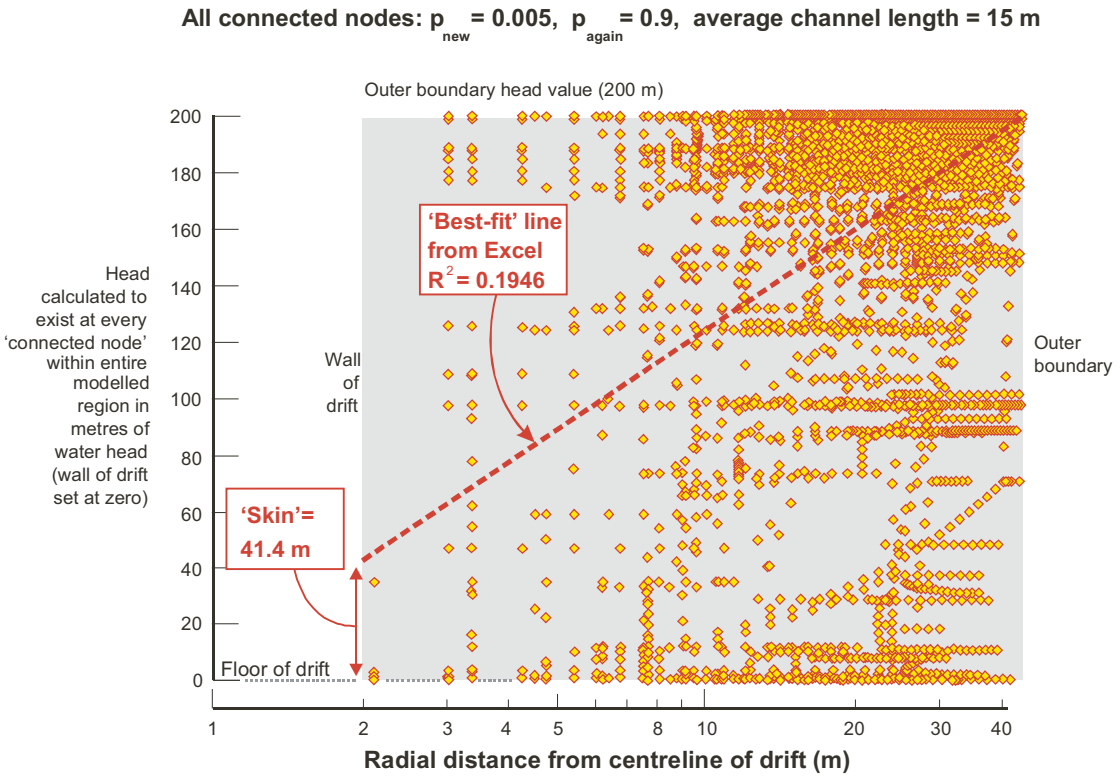

Figure 5-2. *Example of heads versus log radial distance for one realisation of the lattice network model based on 'all connected nodes' and the creation parameters shown. The slope of the best-fit line (118 m) combined with the calculated inflow rate yields a value of K_{rock} 'head fit' 'all nodes'. (An explanation of how to interpret this form of representation accompanies Figure 5-3.)*

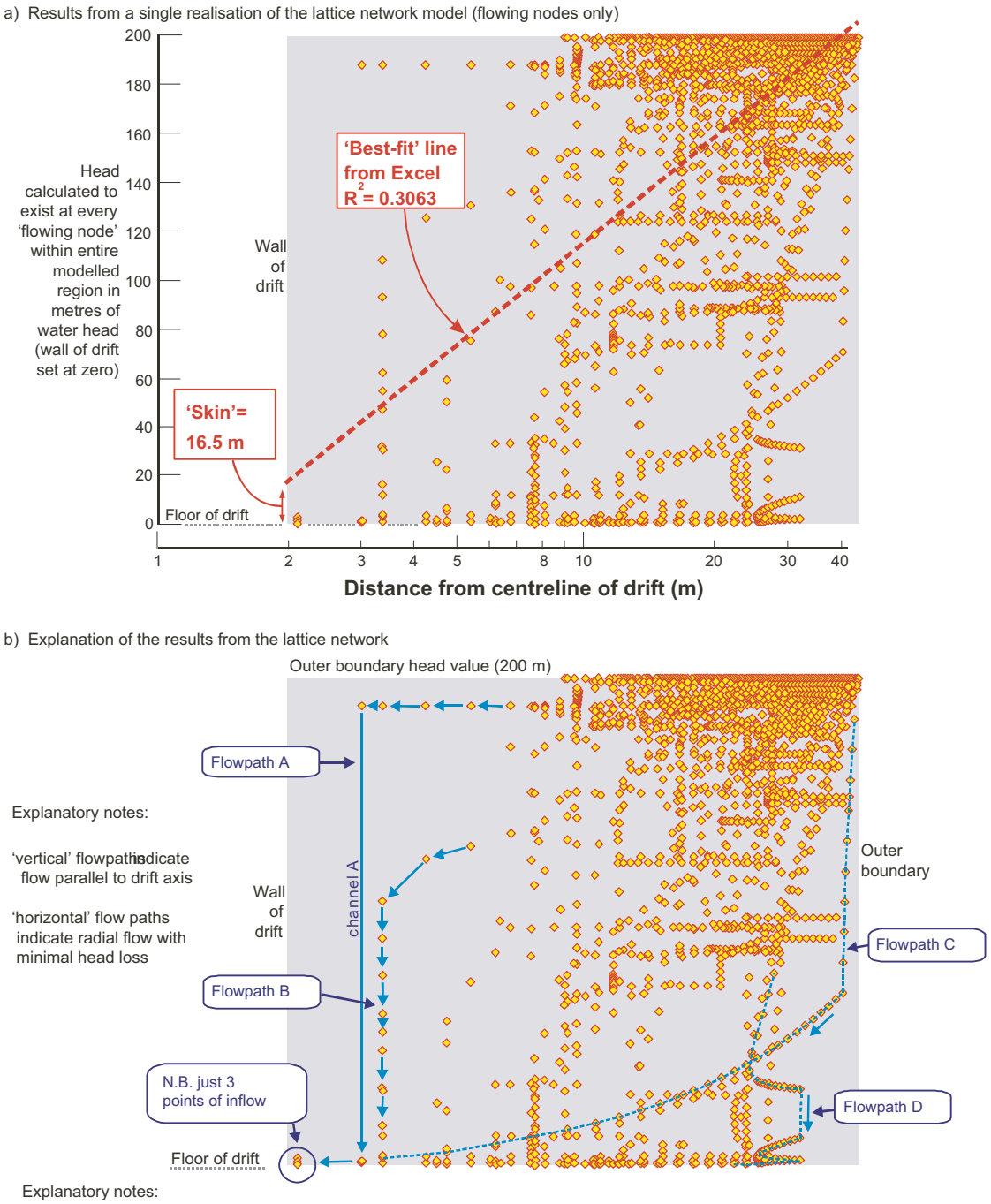

Explanatory notes:

Flowpath A is at ~95% of outer boundary head to within 1m of the drift wall and then loses most of that head in one single low conductance channel (channel A).

Flowpath B loses ~40% of outer boundary head to get to within 1.5 m of drift wall where it then turns and runs parallel to the drift axis for about 10 links (about 15 m).

Flowpath C is mostly made up of a single radial channel that extends almost to the outer boundary. A second channel links to the outer boundary.

Flowpath D loses most head flowing 'around the periphery before linking to a very low head (high conductance) channel about 30 m from the drift wall.

Figure 5-3. *Example of the effect of removing the 'non-flowing' nodes from the realisation in Figure 5-3. NB The value of hydraulic conductivity is increased by 20%, skin effect is reduced from 41 m to 16 m and the goodness of fit is slightly improved. The derived value of hydraulic conductivity is termed K_{rock} 'head fit' 'flowing nodes'.*

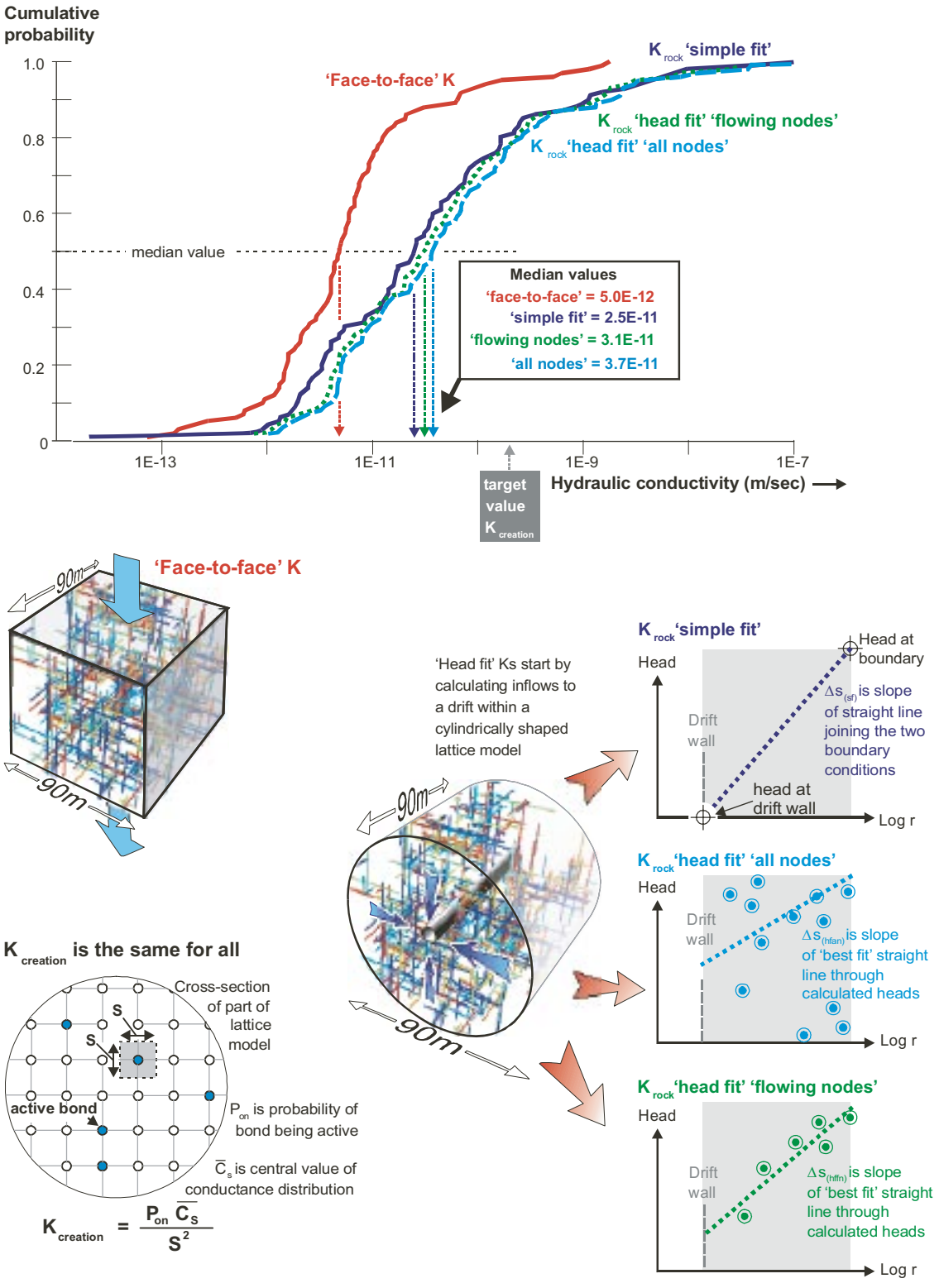

Figure 5-4. *Cumulative Density Function (CDF) distributions for the 100 realisations. Note that only the 'head fit' values of hydraulic conductivity are associated with determinations of 'skin'.*

CDFs are, by definition, based on arranging results in ascending order so that Figure 5-4 says nothing about the relationships between the various calculations of K for a given realisation. This is explored in Figure 5-5, which shows what is evident in Figure 5-4, that all the 'cylindrical geometry based' values of hydraulic conductivity tend to be larger than 'face-to-face' Ks. There is no systematic trend such as lower values of 'face-to-face' K tend to be associated with lower values of 'head-fitting'. A few 'face-to-face' values exceed their counterparts by up to about 3 orders of magnitude but, for the most part, the reverse is true and a few results exhibit an extreme difference of up to 5 orders of magnitude ('f2f'= 1E-13 compared to 'cylindrical' = 1E–8!).

The results seem to reinforce the impression that in 'sparse channel networks', chance has a significant effect and that the behaviour is strongly affected by a few 'connections' acting as 'chokes' on the system.

The next aspect worthy of brief examination is how the value of skin, h_{skin}, is related to other parameters. Skin effect (h_{skin}) is only determined in association with the values of K_{rock} derived from 'best-fitting' heads in the drift inflow simulations. The 'face-to-face' and 'simple fit' derived values do not yield a value of skin effect (see Figure 5-4). It can be seen in Figure 5-4 that the distribution of values of K for the 'head fit' 'all nodes' is very similar to that of the 'head fit' 'flowing nodes'. The 50 percentile values are within 10% of each other. However this is not the case for the values of skin effect.

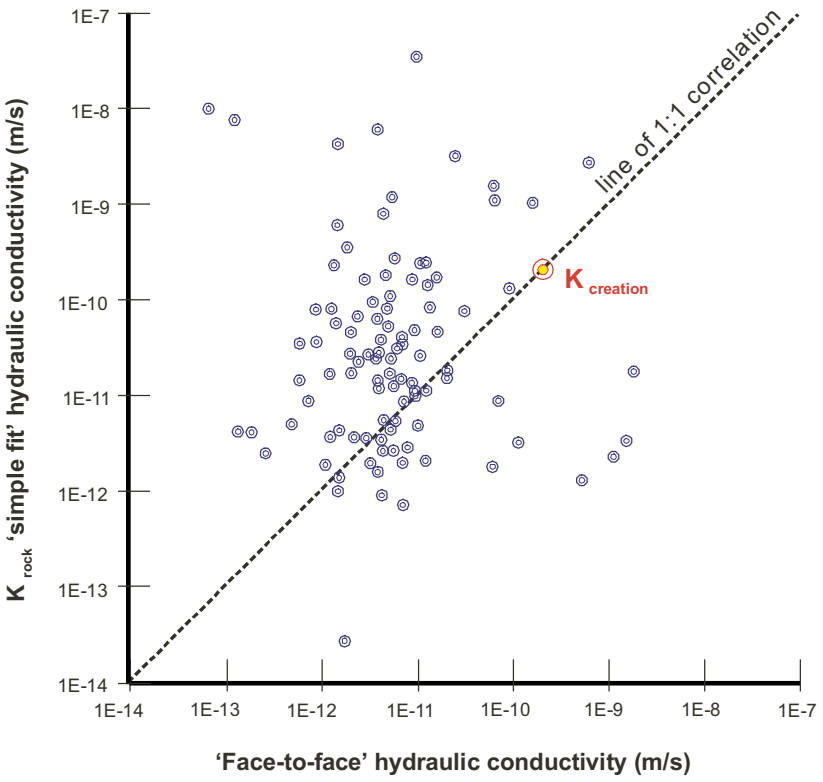

Figure 5-5. *The relationship between the two values of effective large-scale hydraulic conductivity that depend only on the calculation of flow, one across a 90 m cube, the other to the centre of a 90 m diameter cylinder.*

Cumulative plots of h_{skin} for both head-fit results (i.e. 'all nodes' and 'flowing nodes') (see Figure 5-6) show that skin effect is larger in the 'all node' results, with median values of 59 m for the 'all nodes' distribution and 34 m for the 'flowing nodes'. Rather than the 'all nodes' distribution covering a wider spectrum of values, the two distributions simply seem to be offset by about 25 m throughout. Interestingly, roughly 20% of all values are negative. Considering that skin effect cannot exceed +200 m, there are a surprising number of results in excess of 100 m. Values of skin effect in excess of about +130 m are highlighted on Figure 5-6 as 'extreme results' and explained in the inset. It seems likely that in order for the system to be dominated by high heads, there have to be very few low head nodes active in the system, and that therefore there have to be very few inflow points to the central drift. This bears out the analysis of the individual example shown in Figures 5-2 and 5-3.

Comparison of values of skin effect derived from the 'all nodes' and the 'flowing nodes' versions of all 100 realisations (Figure 5-7) shows that, in almost every case, the flowing nodes' result is less than the 'all nodes' result. The difference is therefore systematic.

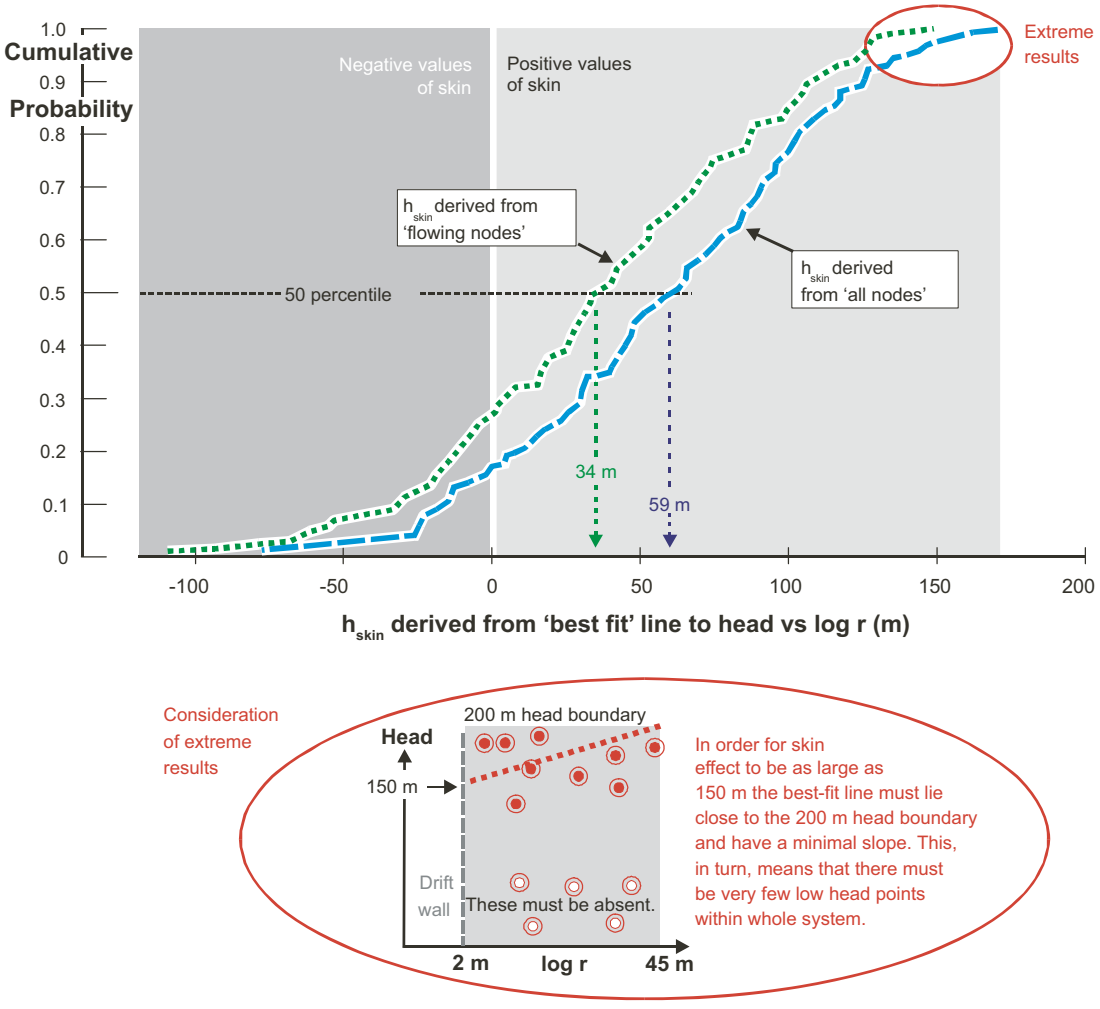

Figure 5-6. *Cumulative Distribution Functions (CDFs) of skin effect (h_{shin}) for both 'head fitting' determinations of hydraulic conductivity from the flow-towards-a-drift configuration of the lattice network model.*

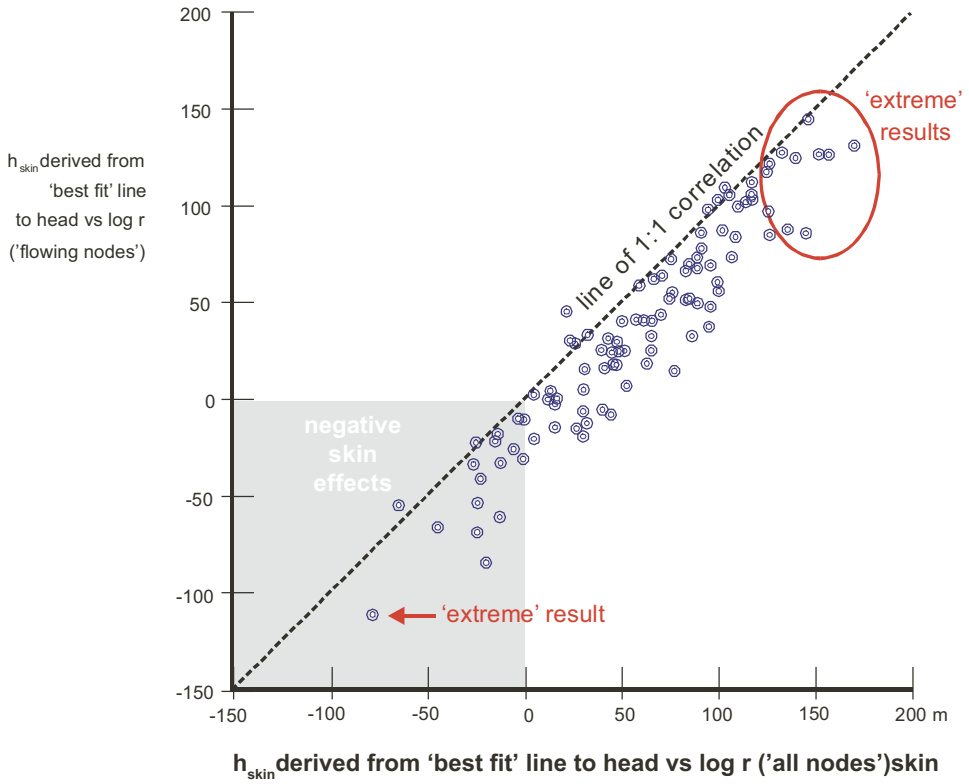

Figure 5-7. *Comparison of skin effect values derived from 'all nodes' and 'flowing nodes' configurations.*

It is probably caused by the nature of the numerical experiment in that the external boundary condition of 200 m head is applied over a much larger area and that it connects to a number of dead-end pathways that approach quite close to the drift. The reasoning is explained within the format of the semi-log plot of head versus log r that is also the source of the value of skin (Figure 5-8).

The effective anchoring of the 'best-fit' line to the 200 m boundary condition at 45 m radius has a second outcome in that the value of skin effect is then linked to the value of hydraulic conductivity. The link is explained in Figure 5-9 and is summarised as Equation 5.1

$$K_{rock} = 0.09q \Big/ (200 - h_{skin}) \qquad (5.1)$$

where q = the calculated inflow to the drift per linear m.

The linkage indicated in Equation 5.1 means that if inflow (q) remains constant then as h_{skin} increases then K_{rock} should also increase. Obviously, the inflow is different in all 100 realisations but assuming that it varies randomly about a central value there should be a general correlation of skin effect and hydraulic conductivity such that higher values of one are associated with higher values of the other. This is examined in Figure 5-10. below which shows that there is no correlation. This, in turn, must mean that higher values of skin are associated, in the lattice model results, with lower values of inflow. It should be borne in mind that variation in the value of inflow is reflected directly in the variability of K_{rock} 'simple fit' since it incorporates a fixed Δs. Figure 5-4 shows K_{rock} 'simple fit' varying over almost 5 orders of magnitude so that must also be the variation in inflow (q). Figure 5-10 shows a similar range of values of hydraulic conductivity so it can be concluded that most of the variability stems from the variation in the values of inflow.

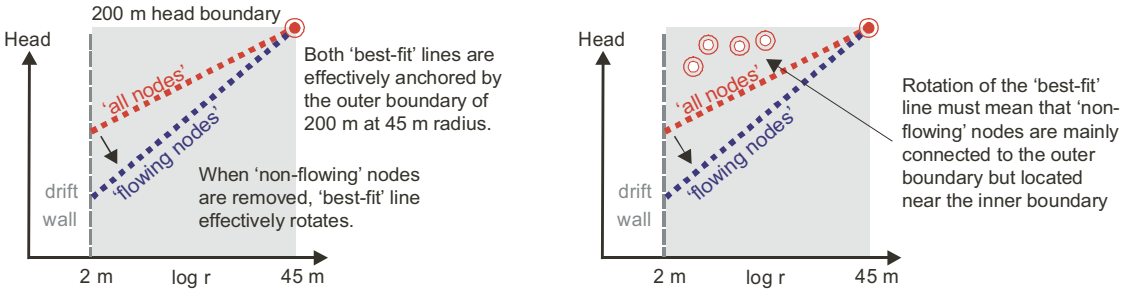

Figure 5-8. *Graphical explanation of where the 'removed' 'non-flowing' nodes must be located in order for there to be a systematically higher skin effect, h_{skin}, in the 'all nodes' results.*

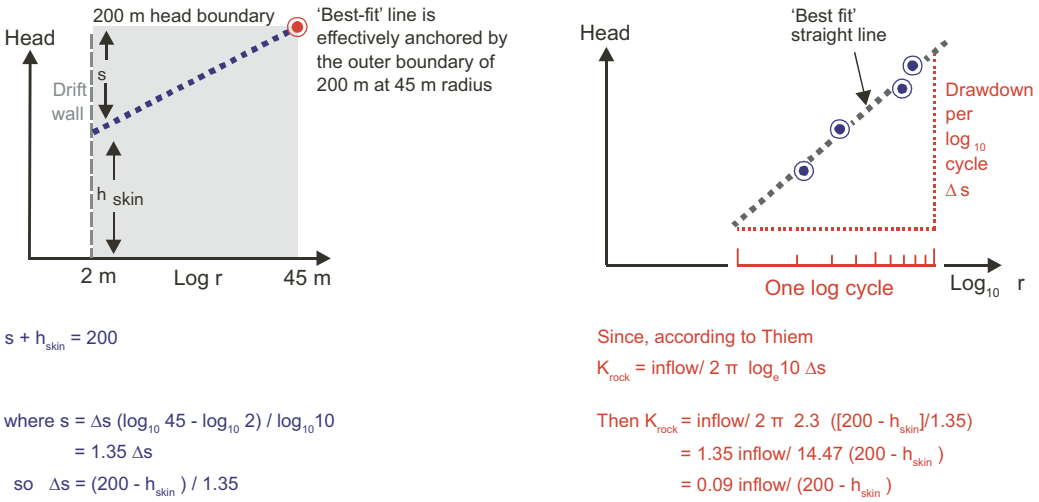

$s + h_{skin} = 200$

where $s = \Delta s (\log_{10} 45 - \log_{10} 2) / \log_{10} 10$

$= 1.35\ \Delta s$

so $\Delta s = (200 - h_{skin}) / 1.35$

Since, according to Thiem

$K_{rock} = \text{inflow} / 2\pi \log_e 10\ \Delta s$

Then $K_{rock} = \text{inflow} / 2\pi\ 2.3\ ([200 - h_{skin}]/1.35)$

$= 1.35\ \text{inflow} / 14.47\ (200 - h_{skin})$

$= 0.09\ \text{inflow} / (200 - h_{skin})$

Figure 5-9. *Explanation of the effective link between the determination of skin effect and hydraulic conductivity.*

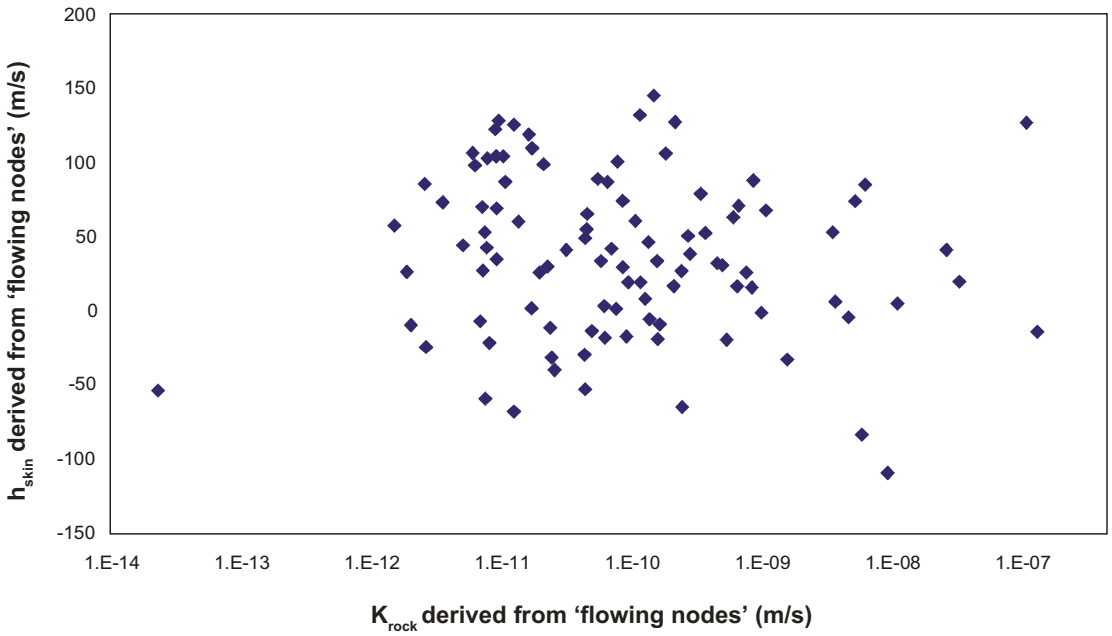

Figure 5-10. *The relationship between determinations of skin effect and hydraulic conductivity for the 100 realisations using the 'flowing nodes' results.*

6 Discussion

6.1 Recognizing flow regimes

The key to understanding the results from the modelling is to recognize flow regimes in the head data. This is because the derivation of the various values of K, except the 'face-to-face' value, is based on assuming that convergent flow to a line sink is an appropriate approximation.

It is best to begin by considering 3 simple flow configurations and assuming flow to a central discharge point.

1. **Linear flow** (flow along a pipe). In constant flow along a pipe towards a central discharge point the transmissivity of the pipe remains constant and so the head gradient remains constant regardless of distance from the source. If the head along a pipe to a central point from an outer boundary were plotted in the same manner as Figures 5-2 and 5-3, then the result would resemble Figure 6-1a below. The curvature is a result of the x-axis being logarithmic.

This head versus distance relationship is quite distinctive and can be seen amongst the results shown in both Figures 5-2 and 5-3 (e.g. the inner portion of Flowpath C on Figure 5-3b).

2. **'Cylindrical flow'.** In constant radial flow towards a central line sink the transmissivity of the system at any given distance from the sink is proportional to the distance from the line sink. In order to maintain constant flow the head gradient must increase proportionally to 1/r. This means that the head in the system should be directly proportional to the logarithm of distance from the sink. A straight line on a plot of head versus logarithm of r is the result (Figure 6-1b). Careful examination of Figure 5-3 does not reveal any part of the system exhibiting this particular behaviour directly.
3. **'Spherical flow'.** In spherical flow towards a central discharge point, the transmissivity of the system at any given distance from the sink is proportional to the distance from the line sink squared. In order to maintain constant flow the head gradient must increase proportionally to $1/r^2$. This means that the head in the system should be directly proportional to 1/r, the inverse of distance from the sink. When such a head relationship is plotted in semi-log form, it should resemble Figure 6-1c. Similarly to cylindrical flow, it is not seen in Figure 5-3. However, if it is occurring within the system being modelled it is unlikely to show in the results because the distance used in the plots is distance from the line sink and not necessarily distance from any specific point, along the line. It should be borne in mind that in order to use the observation of spherical flow behaviour to derive a value of hydraulic conductivity, it is necessary to know the throughflow area somewhere relative to the discharge point. This is not a trivial undertaking.

In summary, linear flow is seen in the results, but cylindrical and spherical flows are not evident. However, it should be borne in mind that the results are neither calculated nor represented in such a way that a spherical flow configuration is likely to be seen. The same cannot be said of cylindrical flow.

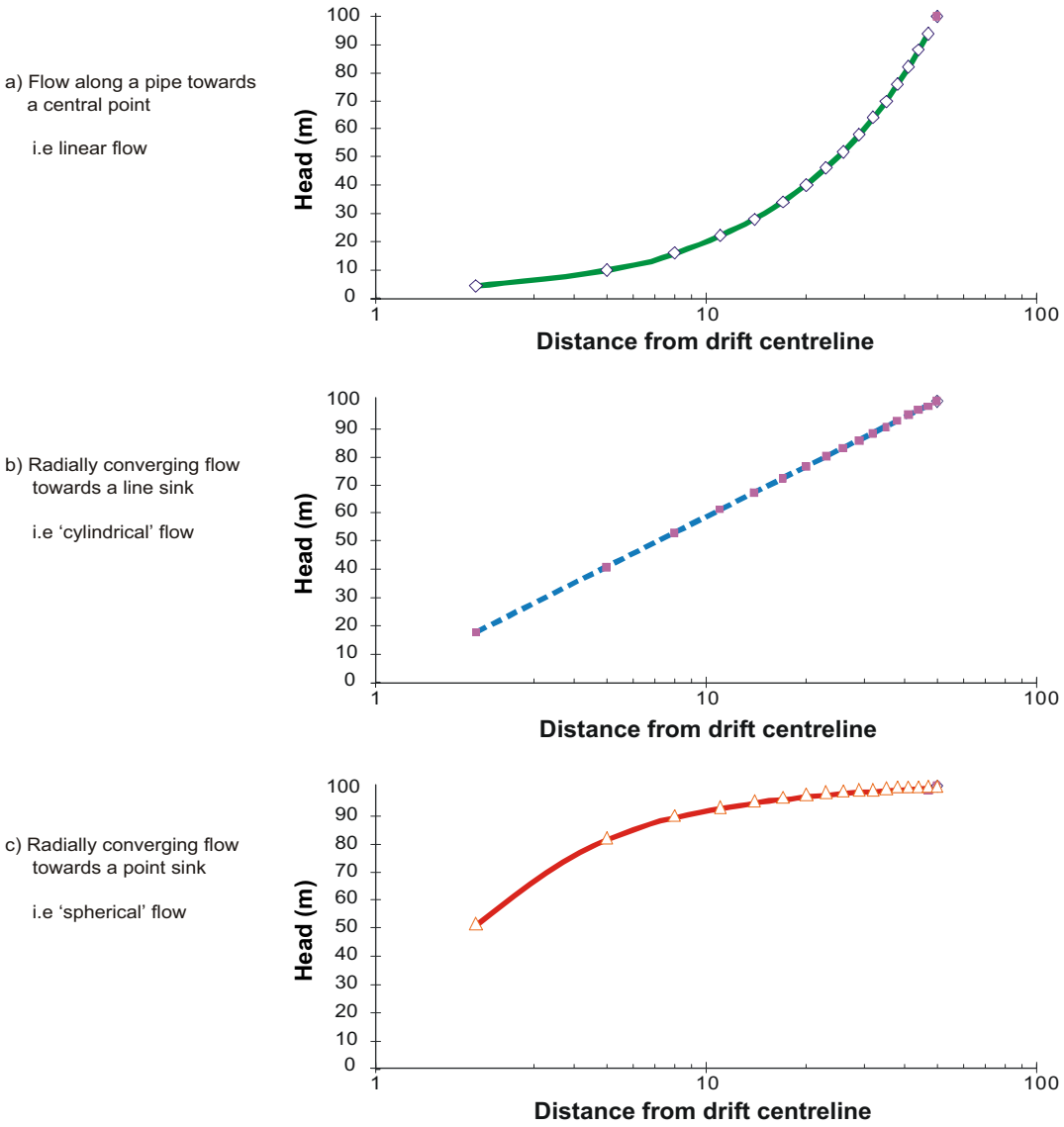

Figure 6-1. *Plots of the head along flowpaths towards 'sinks' of the types specified.*

6.2 Misapplication of the line-sink assumption

It is commonly assumed that flow in a fractured rock will approximate to flow in a porous medium at some scale large enough to include many transmissive fractures. However, the network modelled here is purposely designed to be sparse. In fact, it is unlikely to adopt cylindrical flow symmetry since the inflow is calculated to occur at very specific points. The drift or borehole will behave like a line of point sinks. Hence, a mixture of either linear flows or 'pseudo-spherical'[1] flows is more likely than one involving cylindrical flows.

The results of assuming that either a linear system or a spherical system is cylindrical and applying a line source interpretation to them is revealing (see Figure 6-2).

[1] 'pseudo-spherical' is meant in the sense that a branching network of equal conductances will appear to have a cross sectional area that increases with distance from the source point. Since the branching network occupies a 3D space, it will appear to have a flow dimension somewhere between 1 and 3.

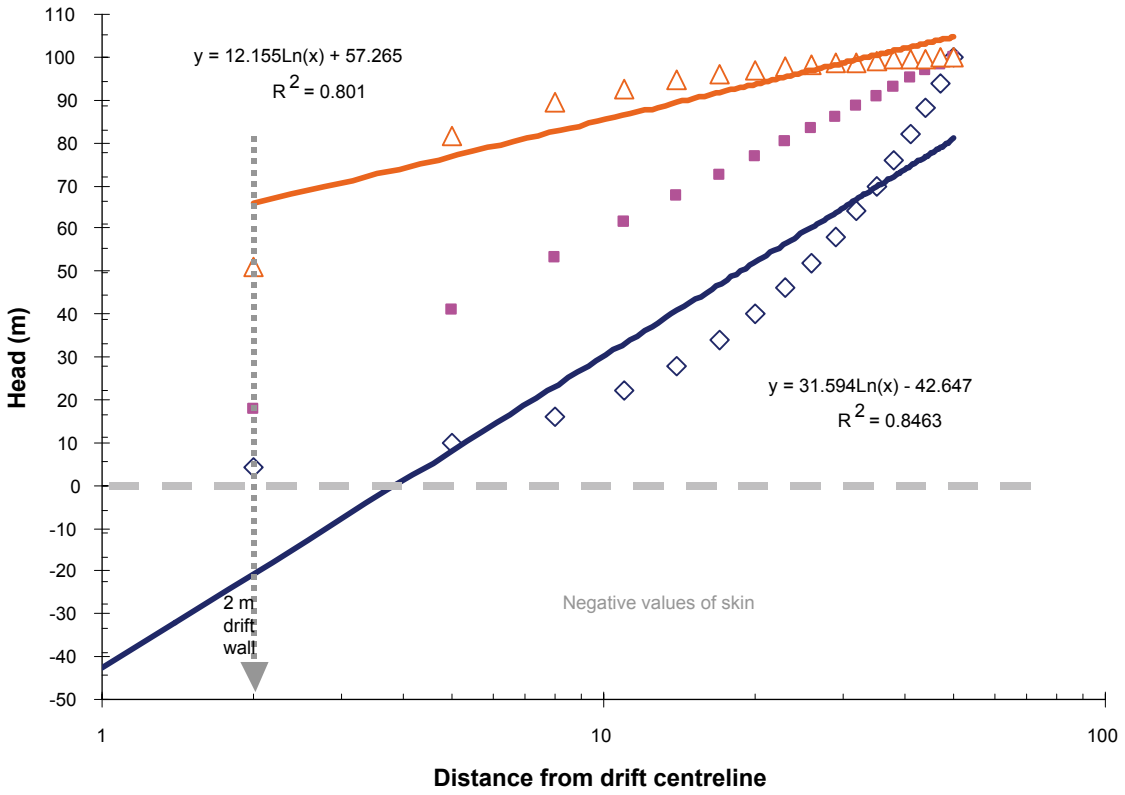

Figure 6-2. *Plot of the best-fit regression lines for the application of a logarithmic relationship of head versus the logarithm of r.*

Figure 6-2 shows that a regression line to data that is essentially spherical will produce a positive skin whereas the best fit to results that reflect linear behaviour is a negative skin. It is especially interesting that the apparent K determined using this interpretative approach will change so that the linear system will appear less permeable than the spherical system. A further aspect is that if data is predominantly from the 'far-field' then, in the case of spherical flow, the determined slope will decrease and apparent K will increase. In the case of linear flow, far-field measurements will sample the 'steep' part of the head plot, large Δs's will result and low values of K coupled with negative skin will be derived. However, the chances of such a single linear pathway being sampled by boreholes from the drift are negligible.

6.3 Is the lattice network model a reasonable representation of the Macro-Permeability experiment?

The lattice network model is not an attempt to represent the actual geometry of fractures or channels in space. Rather, it is a numerical representation that includes some of the geometry that we expect typifies sparse channel networks. Assessing whether it is a reasonable representation of an actual experiment, the Macro-Permeability experiment, is therefore about whether the lattice network exhibits similar behaviour to that which was observed at Stripa. A second aspect that arises is that, although the lattice model realisations were based broadly on the dimensions of the Macro-Permeability experiment, some of the expected 'behaviours' were actually observed in other nearby experiments, such as the '3D Migration experiment'. These 'behaviours' include aspects like very localised inflow such

as was observed in the '3D Migration experiment' and the 'Validation Drift' but not in the Macro-Permeability experiment due to the nature of water removal (i.e. by evaporating the whole surface to dryness). A comparison of 'key behaviours' shows:

- **'Drift scale', inflow-derived hydraulic conductivity of 2×10^{-10} m/sec.**
  The hydraulic conductivity of the rock around the drift was reported by /Gale et al. 1982/, as about 1×10^{-10} m/sec for the Macro-Permeability experiment. It is calculated in this report as having a value of 2×10^{-10} m/sec on Figure 3-3. The median values of the distributions of hydraulic conductivity based on cylindrical flow to a central drift within the lattice model were 2.5×10^{-11} m/sec, 3.1×10^{-11} m/sec and 3.7×10^{-11} m/sec, (for 'simple fit', 'flowing nodes' and 'all nodes' respectively). In other words the model results were about half an order of magnitude less than the experimental values. This was coupled with a 4 orders of magnitude spread in the results.

- **Skin effect in the order of a few tens of metres.**
  The apparent skin effect reported by /Gale et al. 1982/, was 42 m for the Macro-Permeability experiment. The median values of the head-fitting derived values of skin effect from the 100 realisations of the lattice network model were 34 m and 59 m ('flowing nodes' and 'all nodes' respectively).

- **Head variability measured in nearby boreholes.**
  In the Macro-Permeability experiment, the head measurements in the 5 m long sections varied widely. At 40 m from the drift wall, measured heads varied between 50 m and 140 m (Figure 3-1 and 3-3). Heads measured at nodes in the lattice model varied more widely (Figure 5-2 and 5-3) between 0 and 200 m but it should be borne in mind that 'node' values are point calculations whereas boreholes have a natural 'averaging' action. It is interesting to note that, despite the different appearances of the two data sets (Figure 3-3a and Figure 5-3a) the 'R^2' values, denoting goodness-of-fit, were practically the same for both data sets at 0.3.

- **Small number of inflows.**
  The Validation Drift showed that inflow was limited to a small number of areas of the drift wall. In the case of the Validation Drift these amounted to about 6 areas in 50 m length of drift. In the examination of one particular realisation of the lattice network model in Figure 5-3b, it was seen that the modelled drift had only 3 fully connected inflow points in 90 m of drift. This was out of a likely 23 active bonds and 480 potentially active nodes.

- **Flow parallel to the drift axis.**
  /Birgersson et al. 1994/ reported that in the 3D Migration experiment, tracers, injected only 20 m into the roof of their drift later appeared more than 200 m away in their access drift. This implied a significant flowpath parallel to the axis of their drift. In the interpretation of the detailed set of model results shown in Figure 5-3b, 'flowpath B' would appear to be of this type running parallel to the drift for about 15 m.

- **drift-determined value of hydraulic conductivity much less than average of small-scale values.**
  In line with common practice, /Gale et al. 1982/, 'upscaled' their local single-borehole packer tests into a supposedly large-scale value of hydraulic conductivity by taking the geometric mean of the 147 test results. At 9×10^{-10} m/sec this turned out to be about 10× greater than the value derived from the inflow to the drift coupled with the head measurements. In the lattice network case, the average of the small-scale values ($K_{creation}$) was derived differently (see Equation 4.4) but turned out to be about 10× greater than the median values for the determinations based on inflow to the imaginary drift.

It is concluded that flow within a sparse channel network as represented in the lattice network model reproduced all of the key behaviours seen in the Macro-Permeability experiment. Also, some relevant features such as axis parallel flow and very limited inflow points that were observed in experiments nearby (i.e the Validation Drift experiment and the 3D Migration experiment) were also exhibited in the model results.

The following is a description of the experiment based on assuming that the behaviour inherent in the sparse channel model is more or less correct.

The Macro-Permeability drift attracted inflow within discrete yet sparse channels. Flow was probably to a series of point sinks distributed quite sparsely around the walls and floor of the drift. Each behaved as a gathering point for a connected network of channels whose interconnections increased roughly proportionally to distance from the inflow point to a power greater than one. In other words, it had a flow dimension greater than 2. The errors in applying a line sink solution to the observed heads were twofold. Firstly the distances used (zone midpoints) were probably much less than reality because the flow was not conforming simply to distance from the nearest wall but rather to distance from the ultimate individual inflow points. Secondly the decline of drawdown with distance adhered more to spherical than cylindrical geometry and so the rate of rise towards boundary value heads was greater than assumed. In other words, the flow to the drift experienced hyper-convergence, i.e. there was a significant component of spherical flow within the channel network immediately surrounding the drift. With increasing distance from the wall of the drift, the individual inflow-point-based networks probably interconnected and the error arising from using the direct distance to the nearest drift wall declined. Thus at larger distances the flow system began to reasonably approximate cylindrical flow. The near-drift region of ‘hyper-convergence’ was incorrectly identified as ‘skin’ for which an explanation was sought and usually referred to as the ‘Excavation Damage Zone’ (EDZ). It is unlikely that the EDZ is a significant feature in terms of altered fracture or channel transmissivities

Later when the temperature of the ventilating air was raised to increase the overall abstraction rate, the effect was to move the air/water interface further into the wall rock (Figure 3-2). This probably reduced some inflow points to dryness, particularly in the roof and upper walls, and near-drift flowpaths probably became lengthened. This in turn reduced inflow rates.

This is a reasonably simple explanation of groundwater flow in the rock at Stripa, though it does call into question the meaning of hydraulic conductivity as determined in the field and what value should be used in a long-term model. It also raises questions about how K is defined in terms of parameters.

6.4 Evolving concept

This study began with a concept of ‘hyper-convergence’ based on a limited number of inflow points to a drift in fractured rock and embodied in Figure 1-1. It is apparent that Figure 1-1 gives the impression that there are a large number of active fractures in the vicinity of inflow points. This is not borne out by the modelling and a new concept has evolved based on the modelling results. This new concept is shown in Figure 6-3. It is important to recognise the overall sparseness of the channel connection system and the large amount of the geosphere that is likely to be inactive in terms of groundwater flow.

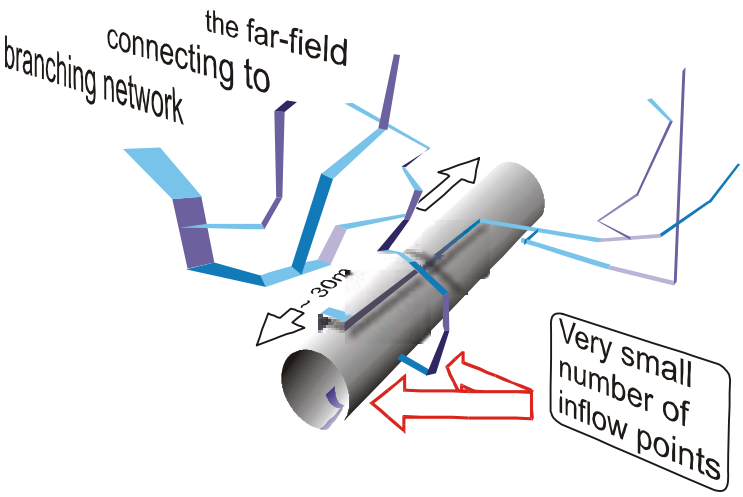

Figure 6-3. *Schematic illustrating the nature of how a sparse channel network probably interacts with a drift.*

6.5 Alternative values of hydraulic conductivity

The Macro-Permeability experiment produced two values for large-scale hydraulic conductivity, the geometric mean of the small-scale tests and the drift inflow based value. They differ by about an order of magnitude. On the other hand, the sparse channel network modelling reported here produces 4, possibly 5, values of overall hydraulic conductivity. Even their median values span 2 possibly 3 orders of magnitude. It is useful to compare them with the experiment values.

Starting at the smallest scale, the single borehole tests of the Macro-Permeability experiment were performed in 2 m (plus some 4 m) long intervals in the 15 boreholes originating from the experimental drift. Each test derived a value of transmissivity that was divided by the length of the test interval to produce a value for hydraulic conductivity. It was assumed therefore that the value from each test represented the hydraulic conductivity of a small volume of rock and fractures. Since the rock is not systematically layered or fractured into regular blocks, the individual volumes were assumed to be randomly spatially organised and a geometric mean taken to represent the large-scale overall behaviour.

The equivalent in the network modelling to constructing large-scale behaviour from small-scale measurements is the target value ($K_{creation}$) concept in the creation of the network whereby local values of conductance are sampled from a log normal distribution. Because of the lattice spacing (1.5 m) each conductance applies over a unit volume so can be seen as a local hydraulic conductivity. The target value of effective large-scale hydraulic conductivity is arrived at by assuming that the 'inactive' nodes of the system are volumes of zero hydraulic conductivity. However in the realisations presented, there are over 20 times more local values of zero hydraulic conductivity than there are positive values. The outcome of this process is that, whilst the central value of the small-scale hydraulic conductivity distribution is 4.2×10^{-9} m/sec the average value for the created lattice network is 2×10^{-10} m/sec.

The next scale up in terms of the size of region modelled or measured is the 'drift scale'. In the Macro-Permeability experiment, this had a single value of about 1×10^{-10} m/sec. The equivalent in the lattice network modelling was three distributions of results derived from combinations of inflow calculations and head measurements. The three, here termed 'simple fit', 'head fit flowing nodes' and 'head fit all nodes', all produced very similar results with

median values of 2.5, 3.1 and 3.7×10^{-11} m/sec (Figure 5-4). Hence, in both experiment and in modelling, the value of hydraulic conductivity based on inflow to a drift was about a tenth of the value derived by 'upscaling' small-scale measurements.

The final value to be considered is the model-based 'face-to-face' hydraulic conductivity. It is interesting for several reasons. Firstly, the cumulative distribution is 'steeper' than the 'head-fit' distributions (see Figure 5-4) showing that it forms a narrower frequency distribution (Figure 6-4) than the others especially the distribution of conductances that

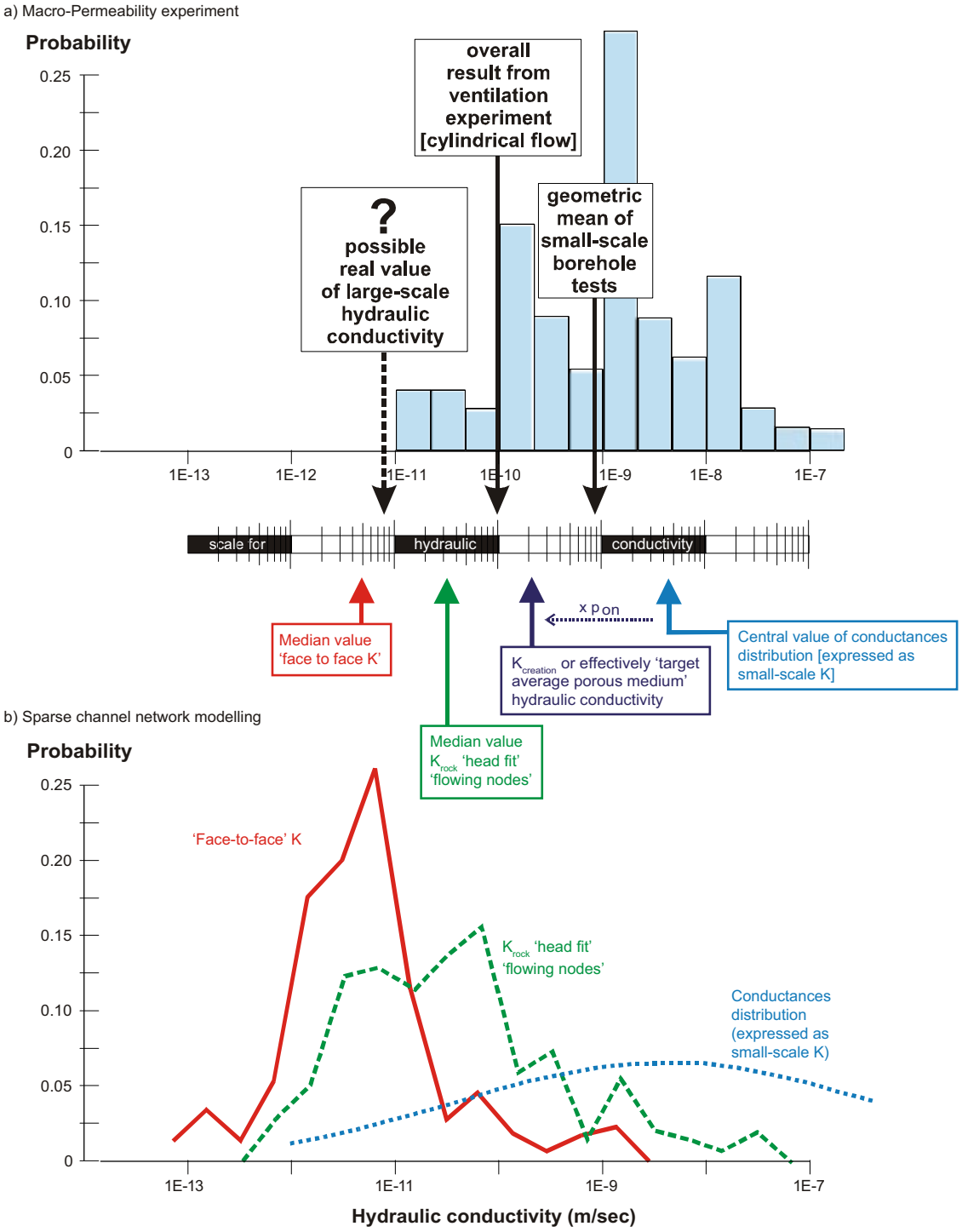

Figure 6-4. *Comparison of the results from the Macro-Permeability experiment with those from the sparse channel network modelling.*

was used in model formation. Secondly, the median of the 'face-to-face' distribution is almost a whole order of magnitude less than the 'drift-scale' values. Finally, it must be assumed that, for 80% of values to be more than an order of magnitude less than the 'creation' value, low conductance linkages must dominate the results. This feature was already identified in the results of the 'cylindrical' flow modelling but, for some reason, it appears more important in the parallel flow field assumption of the 'face-to-face' results. Perhaps it is because the cuboidal version of the model requires flowpaths to be twice as long as in the cylindrical version.

Whatever the reason for it, there appears to be roughly 3 types of hydraulic conductivity in the model results, upscaled small-scale values, drift-scale (misapplied cylindrical flow concept) values and 'large-scale' ('permeameter style') values, each approximately a tenth of the value of the next smaller scale. If this is real then the Macro-Permeability experiment failed to measure the actual 'large-scale' hydraulic conductivity which might have a value about 1×10^{-11} m/sec (as suggested on Figure 6-4).

This would have important implications for predicting repository performance on the basis of current in-situ field test methods.

The large-scale value might perhaps be seen in the field through the mechanism of the mixing of bodies of groundwater over very long timescales, in other words via differences in hydrochemistry.

6.6 Other implications of a sparse channel model

6.6.1 Basic attributes of a sparse channel network

The basic attributes of a sparse channel network are:

- The individual channels are significantly elongated in one direction with aspect ratios in the order of 10:1 or more.
- The highly non-equidimensional channels have a moderate frequency of occurrence but a low chance of interconnection so that the overall network is close to the limit of percolation.

These basic attributes give rise to a number of characteristic behaviours, of which 'hyper-convergence' around drifts and boreholes is one. The others are also consequences that are observable in field experiments.

6.6.2 Compartmentalization

It appears from the results of this study that the large-scale behaviour of many of the network realisations was dominated by a few low conductance connections. In other words, flow through the network was controlled by a few 'choke' points. The corollary of a few 'choke' points is that the rest of the active network will allow the small flows controlled by the 'choke' points to flow through with minimal head loss. This gives rise to a system with sizeable regions all at similar head connected to the rest of the system through individual channels in which the bulk of head loss occurs. Hence flow through the network would be analogous to a river that consisted almost entirely of lakes separated by waterfalls. Thus

when examining the heads measured in such a system one would expect to find certain head values are very common whilst others seldom register. There is some evidence of this type of behaviour in the results shown in Figure 5-3 with certain values of head (i.e. 88–89, 105–110 and 130–132) occurring particularly frequently. Compartmentalisation is noted in work published by /Sawada et al. 2000/, about Kamaishi, and by /Poteri et al. 2002/ (pages 103–111), about the Äspö TRUE Block Scale experiment.

6.6.3 Borehole involvement in the flow system

In the network modelling reported here, the number of inflow points to the central drift is small. Three points are seen in the example examined in Figure 5-3. It should also be borne in mind that, on the basis of the 6 central boreholes of the Simulated Drift Experiment apparently acting to some extent hydraulically independently; it was decided to envisage channels that could fit between boreholes less than 1.5 m apart. Hence in the model, channels are seen as quite small; say about 15 m long, less than 1.5 m wide and with a most likely aperture of about 20 to 30 microns. It is not difficult to imagine that boreholes in the order of 50 m long with a diameter of 76 mm and practically infinite conductance are extremely significant pathways within such a sparse system. It should also be borne in mind that the model was designed to have 95% of all nodes (representing 95% of the space) inactive. Overall then, it should be anticipated in sparse channel networks that investigation boreholes participate in the natural flow system even when divided into shorter lengths by packers for monitoring.

Evidence of investigation boreholes participating in the natural flow system is not recorded directly by any authors. However, the Simulated Drift Experiment of the Stripa Project placed six 100 m long boreholes in close proximity and allowed them to flow throughout their entire length (See Appendix A for detailed description of events and results.). The result was that the multi-borehole system allowed almost 10 times more inflow than the subsequent drift and, at about 2×10^{-9} m/sec, yielded a bulk hydraulic conductivity about 10× higher than the subsequent drift and the nearby Macro-Permeability experiment.

Another experiment that seems to show evidence of borehole participation is the Äspö TRUE Block Scale experiment where boreholes, which emanate from the access drift, seem to propagate the low head of the access drift across the 200 m extent of the experimental volume (Figure 6-5). (Results adapted from /Dershowitz et al. 2003/.)

In summary, participatory boreholes seem extremely likely in sparse channel networks but conclusive evidence is not available. There are some indications that the apparently anomalous flow behaviour of the Simulated Drift Experiment may be caused by participatory boreholes as also the head pattern of the TRUE Block Scale Experiment.

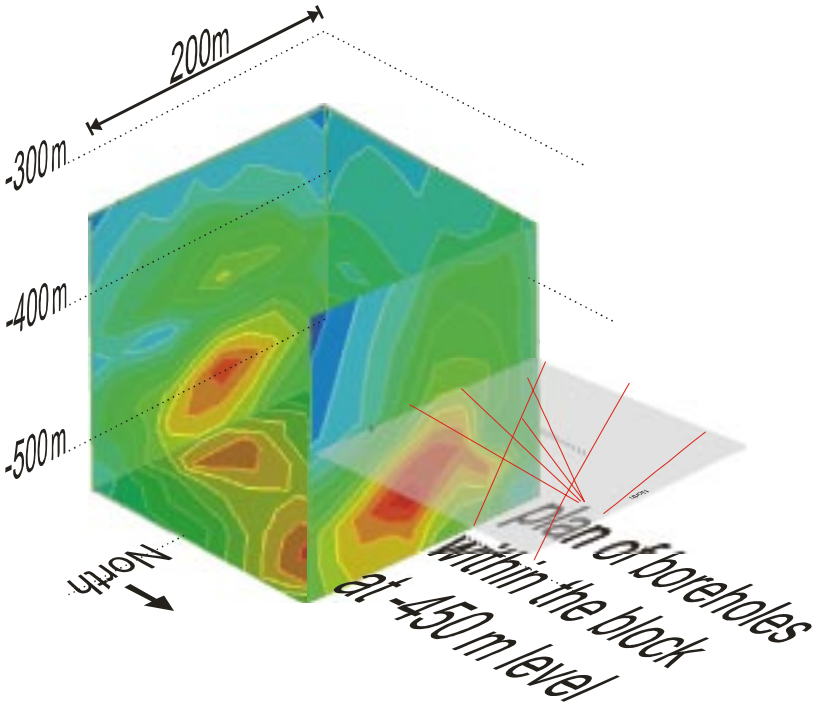

Figure 6-5. *Head conditions interpolated from borehole measurements in the TRUE Block Scale experimental volume. Red is low head, blue is high. NB The access drift is located on the northern face of the block at about 450 m below ground. The boreholes slope slightly downwards towards the opposite face of the test volume. The borehole plan has been placed outside the block for purposes of clarity.*

6.7 Why is this behaviour not seen in existing discrete fracture network and channel network models?

Discrete fracture network (dfn) models have been used for a number of years to model fracture systems at Stripa, Äspö and many other crystalline rock locations with similar conditions. It is likely that they always produce a fracture network that is well connected. This derives from their use of equidimensional fractures. Consider that if two non-parallel, equidimensional fractures are extended towards infinite size they have a 100% chance of intersection. Alternatively, two non-equidimensional, non-parallel fractures with a fixed width have a less than 100% chance of intersection even if extended to infinity. It is the much lower chance of intersection in a channel network that has enabled this work to examine the behaviour of sparse networks close to the percolation threshold. Up until now, most channel networks have been adaptations of dfn models and channels are distributed relatively evenly on pre-existing equidimensional fracture surfaces thus negating one of the properties of channels.

6.8 The Excavation Damaged Zone (EDZ)

The near-field region, that is the rock within a drift diameter of the drift surface, contains the Excavation Damaged Zone (EDZ). Rock mechanics conceives it as a region of enhanced fracture opening and hence increased hydraulic conductivity and hydrogeologists as a skin of reduced conductivity. In a recent review by /Black and Barker 2002/, it was shown that there have been no clear-cut measurements of changed fracture hydraulic properties within the EDZ. Blast damage has been seen to alter the matrix rock but once more than a few centimetres into the drift wall even this effect diminishes to zero. Most of the hydraulic 'evidence' for a zone of altered fracture properties comes from the Macro-Permeability experiment described here and the Rock Sealing Project reported by /Börgesson et al. 1992/. The Rock Sealing Project produced the results of enhanced near-field hydraulic conductivity together with an axially enhanced anisotropy ratio of 40× based on non-unique porous-medium finite element modelling designed and modified to explain a set of very complex results.

The sparse channel modelling here seems to demonstrate that the EDZ should be regarded rather differently from a hydraulics viewpoint. Most importantly, it would appear that the EDZ contains only very small numbers of through-flowing channels that give rise to inflow in a drift. Notably, the sparse channel modelling does not reduce the number of channels or their conductance in the vicinity of drifts and yet still reproduces the 'hyper-convergent' behaviour of the right sort of magnitude. Intuitively, one suspects that the few channels that traverse the EDZ are virtually unaffected by the stress changes in the drift wall because they are not very planar and are orientated predominantly parallel to the major stress direction. The idea of a region of axially enhanced hydraulic conductivity, as concluded in /Börgesson et al. 1992/, would counteract 'hyper-convergence' since it would make any drift appear more like a genuine line sink rather than the cause of hyper-convergence, which is a line of isolated point sinks.

It is concluded that the most likely interpretation of the EDZ is that it is a zone that the few active channels, which control overall inflow to a drift, traverse with little or no alteration. This infers that the conclusions by /Börgesson et al. 1992/, about the hydraulic conditions in the EDZ, based on porous medium modelling, are incorrect.

7 Conclusions

The work reported here was originally intended as an investigation of the phenomenon termed 'hyper-convergence' but has evolved into a study of the cause of 'hyper-convergence', namely, flow through sparse channel networks. In the event, it is clear that understanding flows in fractured crystalline rock in terms of sparse channel networks has profound implications for many aspects of repository investigation, design and performance assessment.

'Hyper-convergence' was originally proposed by /Black and Barker 2002/, to explain the pattern of heads observed near an experimental drift at Stripa in the early 1980's. Subsequent experiments at Stripa developed practical ways of determining the rates of inflow in specific areas of wall rock and enabled the conclusion that inflows to drifts were sparse and very localised. Since the experiments assumed in their design that flow converged radially to the line sink represented by the experimental drift, extra convergence, axially, to the points of inflow was termed 'hyper-convergence'. Effectively, 'hyper-convergence' is flow within a network where the flow 'dimension' is greater than 2, based on a single small area of inflow to a drift as the starting point. A number of geometrical configurations could potentially reproduce such an effect but the interaction of a drift with a channel network was considered the most likely. A lattice network model incorporating concepts of long thin fractures and very low frequencies of occurrence was developed specially to test the idea.

It is concluded that it is straightforward to generate sparse channel networks that demonstrate 'hyper-convergence' in the immediate vicinity of a simulated drift. It is useful to view 'hyper-convergence' as a symptom of how badly flow in a network connected to a line sink adheres to the assumption of 'cylindrically convergent' flow. Flow does not conform to the cylindrical assumption for two reasons:

- The network of channels branches frequently enough such that conductance increases more rapidly with distance than direct proportionality.
- The use of values of distance based on the minimum distance from the drift wall to the point of head observation is invariably an underestimate and frequently a large one.

These are the two main reasons that the commonly used 'semi-log r' representation to derive values of apparent large-scale hydraulic conductivity produces erroneous results. This conceptual and interpretational error causes two problems. The values of hydraulic conductivity are wrong and the concept of skin is invoked.

The work reported here shows that it is comparatively simple to create a sparse channel network based on a lattice network. Early realisations based on very infrequent active bonds, predominantly 10:1 aspect ratios for fractures, a width scale in the order of 1.5 m, and a broad distribution of conductances (log normal with a standard deviation of 2 orders of magnitude), quickly started to reproduce the apparent skin effects seen in the field data. The behaviour of 100 realisations of a single set of creation parameters was examined in detail. They showed that outcomes were extremely variable both in terms of derived hydraulic conductivity and of apparent skin. Hydraulic conductivity ranged over 3 or 4 orders of magnitude and skin ranged from negative values to values almost equal to the outer head boundary.

The main direct conclusions from the modelling were that:

- There were only a small number of inflow points to the modelled drift.
- There was no direct relationship between derived hydraulic conductivity and skin effect.
- The modelling reproduced the key features of the Macro-Permeability experiment.
- The meaning and validity of the value of hydraulic conductivity derived from a drift inflow experiment are very uncertain.

The modelling included a target hydraulic conductivity ($K_{creation}$) that was used to control the variability of conductances used in model creation. It was effectively an upscaling of the collective small-scale values. Subsequent calculations involved a cylindrical version of the lattice network that produced 3 'drift-scale' values of hydraulic conductivity and a cuboidal version that produced a 'large-scale' value. Thus each realisation of the model was associated with 5 values of hydraulic conductivity. As it turned out, the 'drift-scale' values were all quite similar so that effectively there were 3 values each appropriate to a different length scale: small, medium and 'medium-large'. Each one differed by about a factor of 10. If this reasoning is compared to the field values then it appears that what has been measured are the two smaller scale values and that the true large-scale value for Stripa is another order of magnitude less than previously thought. This would also be the case for other sites where sparse channel networks apply.

The main indirect conclusions from this modelling project are:

- That sparse channel networks can be expected to produce 'hyper-convergence' and that where skin effects are apparently observed then a sparse channel network system should be assumed.
- That sparse channel networks can be expected to produce compartmentalisation in the head regime surrounding any natural or artificial flow system such as an excavation or a mine. This is because a few low conductance connectors are the effective controls on the overall flow system.
- That exploration boreholes into sparse channel networks can be expected to be active participants in the system they are being used to observe.
- That EDZs are largely fictitious in terms of altered hydrogeological properties except at the microscopic scale. There is no evidence of an Excavation Damaged Zone of enhanced hydraulic conductivity.

In conclusion, it can be seen that what began as a search for an explanation of a feature of a 20 year old underground experiment turned into a re-appraisal of many concepts that are familiar and well established. In general, it seems like this investigation has taken us into the middle of a new way of understanding fractured crystalline rocks. It would appear valuable to go 'backwards' to understand some of the fundamental principles as well as forwards using more realistic representations of the real world. Some initial ideas are briefly outlined in Appendix C.

There is a pressing need to understand the nature and meaning of hydraulic conductivity in sparse channel networks.

8 References

Birgersson L, Neretnieks I, Widén H, Ågren T, 1994. In-situ Tracer Experiments in Fracture Zones and Averagely Fractured Rock. Proc. Of the 4th International NEA/SKB Symposium, Stockholm. 14–16 October 1992, "In Situ experiments at the Stripa Mine" Publn. of the OECD pp 171–194.

Black J H, Barker J A, 2002. Excavation damaged zones of repositories: their hydrogeological significance and measurement. Report to Quintessa Japan for Japan Nuclear Fuels. Report of In Situ Solutions No. ISS 2002-3, 67 pp.

Börgesson L, Pusch R, Fredriksson A, Hökmark H, Karnland O, Sandén R, 1992. Final report of the Rock Sealing Project. Identification of zones disturbed by blasting and stress release. OECD/NEA International Stripa Project. SKB TR-92-08. Svensk Kärnbränslehantering AB.

Dershowitz W, Winberg A, Hermansson J, Byegård J, Tullborg E-L, Andersson P, Mazurek M, 2003. Äspö Hard Rock Laboratory: Äspö Task Force on modelling of groundwater flow and transport of solutes: – Task 6C – A semi-synthetic model of block scale conductive structures at the Äspö HRL. SKB IPR-03-13, 126 pp. Svensk Kärnbränslehantering AB.

Gale J E, Witherspoon P A, Wilson C R, Rouleau A, 1982. Hydrogeological characterisation of the Stripa site. Proceedings, Geological disposal of radioactive waste – In-situ experiments in granite, OECD/NEA Workshop, Stockholm, Sweden, Oct 25–27, 1982.

Goodman R E, Moye D G, van Schalkwyk A, Javandel I, 1965. Ground water inflows during tunnel driving. Eng. Geology 2, No 1, pp 39–56.

Harding W, Black J, 1992. Site Characterization and Validation – Inflow to the Validation Drift. Technical Report of the Stripa Project, managed by Swedish Nuclear Fuel and Waste Management Co on behalf of OECD/NEA. SKB TR-92-14, 84 pp. Svensk Kärnbränslehantering AB.

Holmes D C, Abbott M, Brightman M A, 1990. Site Characterization and Validation – Single borehole hydraulic testing of 'C' boreholes, Simulated Drift Experiment and small-scale hydraulic testing, Stage 3. Technical Report of the Stripa Project, managed by Swedish Nuclear Fuel and Waste Management Co on behalf of OECD/NEA. SKB TR-90-10, 161 pp. Svensk Kärnbränslehantering AB.

Lei S, 1999. An analytical solution for steady flow into a tunnel. Ground water Vol. 37, No. 1, pp 23–26.

Olsson O (ed), 1992. Site Characterization and Validation – Final Report. Technical Report of the Stripa Project, managed by Swedish Nuclear Fuel and Waste Management Co on behalf of OECD/NEA. SKB TR-92-22, 184 pp. Svensk Kärnbränslehantering AB.

Poteri A, Billaux D, Dershowitz W, Gomez-Hernandez J J, Cvetkovic V, Hautojärvi A, Holton D, Medina A, Winberg A, 2002. Final report of the TRUE Block Scale project. SKB TR-02-15, 230 pp. Svensk Kärnbränslehantering AB.

Rouleau A, Gale J E, 1982. Characterization of the fracture system at Stripa. Report Series of Lawrence Berkeley Lab. Rep. No. LBL-14875.

Sawada A, Uchida M, Shimo M, Yamamoto H, Takahara H, Doe T W, 2000. Non-sorbing tracer migration experiments in fractured rock at the Kamaishi Mine, Northeast Japan. Engineering Geology, Vol. 56, Issues 1–2, pp. 75–96.

Witherspoon P A, Wilson C R, Long J C S, Galbraith R M, Dubois A O, Gale J E, McPherson M J, 1981. Mesures de perméabilite en grand dans les roches cristallines fracturées. Bull. B.R.G.M., III(1), pp 53–61.

Appendix A

Evidence of channel separation and channel size from the experiments at Stripa

A.1 Channel size and separation

The only real evidence for channel separation at Stripa is from the Simulated Drift and the Validation Drift. The Simulated Drift measurements are described in part in main text and consisted of 3 steps of drawdown in the 6 'D' boreholes before excavation. The original intention of the experiment was to match the inflows seen in the boreholes to equivalent inflows measured on the surface of the subsequently excavated drift. For this reason, a measurement system was devised that allowed individual segments of boreholes to be measured whilst also allowing all the rest of the boreholes to continue to flow. The system comprised a manifold to connect all the boreholes to a flowmeter and also apply back-pressure. Thus individual whole borehole flows were measured at 3 different common back pressures. Whilst the overall experiment was going on, an additional straddle packer system was installed in each borehole in turn to measure the inflow into individual sections of the borehole. It was configured in such a way as to measure flow into a section whilst allowing throughflow from the rest of the borehole. The system included a sealable gland at the mouth of the borehole to allow movement of the straddle packer system whilst maintaining pressure in the borehole (see /Holmes et al. 1990/). The results in terms of whole borehole inflows at the three pressure steps and the distribution of inflows along all the boreholes for the largest drawdown step (about 210 m of drawdown) are shown in Figures A1-1 and A1-2.

Figure A1-1 shows the 6 'D' boreholes in cross section with the total individual borehole flow represented as a circle centred on the borehole location. It is apparent that the central borehole continues to attract inflow even when the drawdown is at the maximum value of 210 m. This is surprising given that it could have been expected that the 5 circumferential boreholes would have formed a complete barrier of interlocking regions of reduced head that should have intercepted all flow. The continuation of discharge from D1 indicates that the flow within the rock is channellised and that the channels are capable of 'fitting in between' the circumferential boreholes that are 1.7 m apart. The inflows were also noted to be unstable in as much as sometimes when the straddle packers were inflated inflow rates to the other boreholes altered. On one occasion during Step 3, borehole D3 went from zero flow to 400 l/min when the packers were inflated in D3.

The distribution of inflows along the length of the D boreholes (Figure A1-2) is clearly organised into two groups where they intersect the two so-called fracture zones 'B' and 'H' roughly at 30 m and 90 m. It should be borne in mind that the flow rate axis is linear and the minimum measurement was 8×10^{-4} litres/min.

After the Validation Drift had been excavated, the remaining 50 m of all the 'D' boreholes were retested using similar equipment but with a lower flow measurement limit of 1×10^{-4} litres/min. The results were reported in /Harding and Black 1992/ and were depicted using a logarithmic axis for inflow rate. They are reproduced below with inflow points identified based on the expert judgement of the authors of this report. No account is taken of inflow magnitude except in as much that values need to exceed the minimum measurement limit. Hence based on Figure A1-3, 300 m (6 boreholes each 50 m long) of 75 mm diameter borehole intersected 20 flowing features (channels). That is, about one every 15 m.

Location of boreholes
in cross section

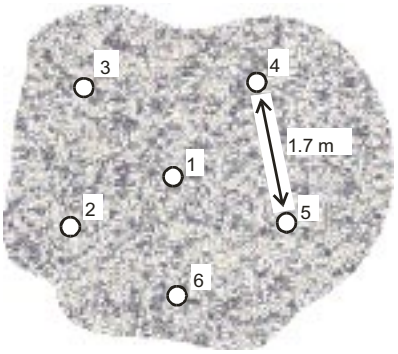

Step 1: drawdown = 79 m
all-hole inflow = 0.73 l/min

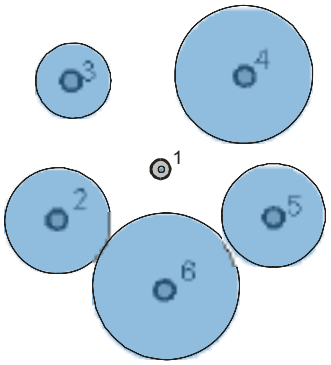

Step 2: drawdown = 157 m
all-hole inflow = 1.34 l/min

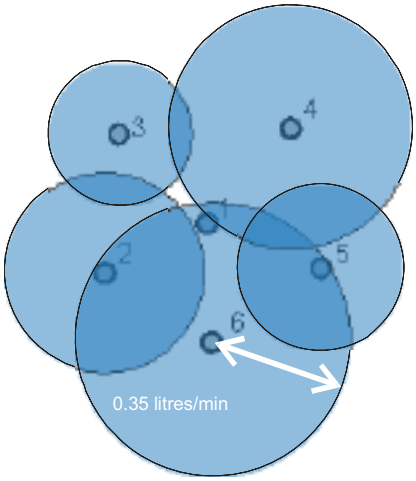

Diameter of circle is
proportional to inflow rate

Inflow to D3 borehole was reduced to zero
in results because it was thought to be
inflow 'diverted' from other boreholes

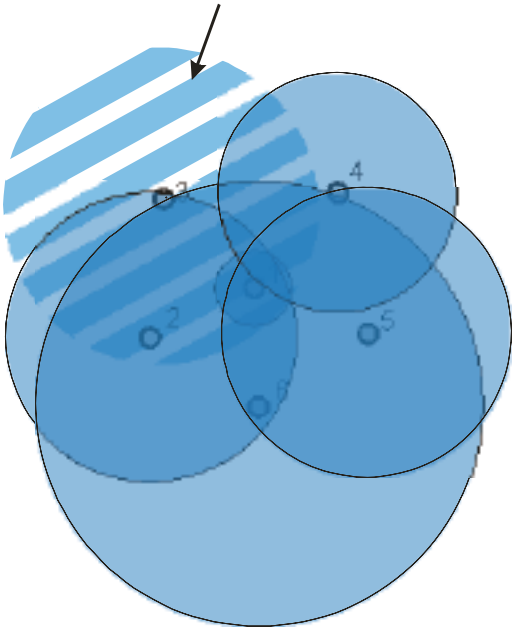

Step 3: drawdown = 210 m
all-hole inflow = 1.71 l/min

Figure A1-1. *The location of the totalised inflows to the 'D' boreholes as part of the Simulated Drift experiment.*

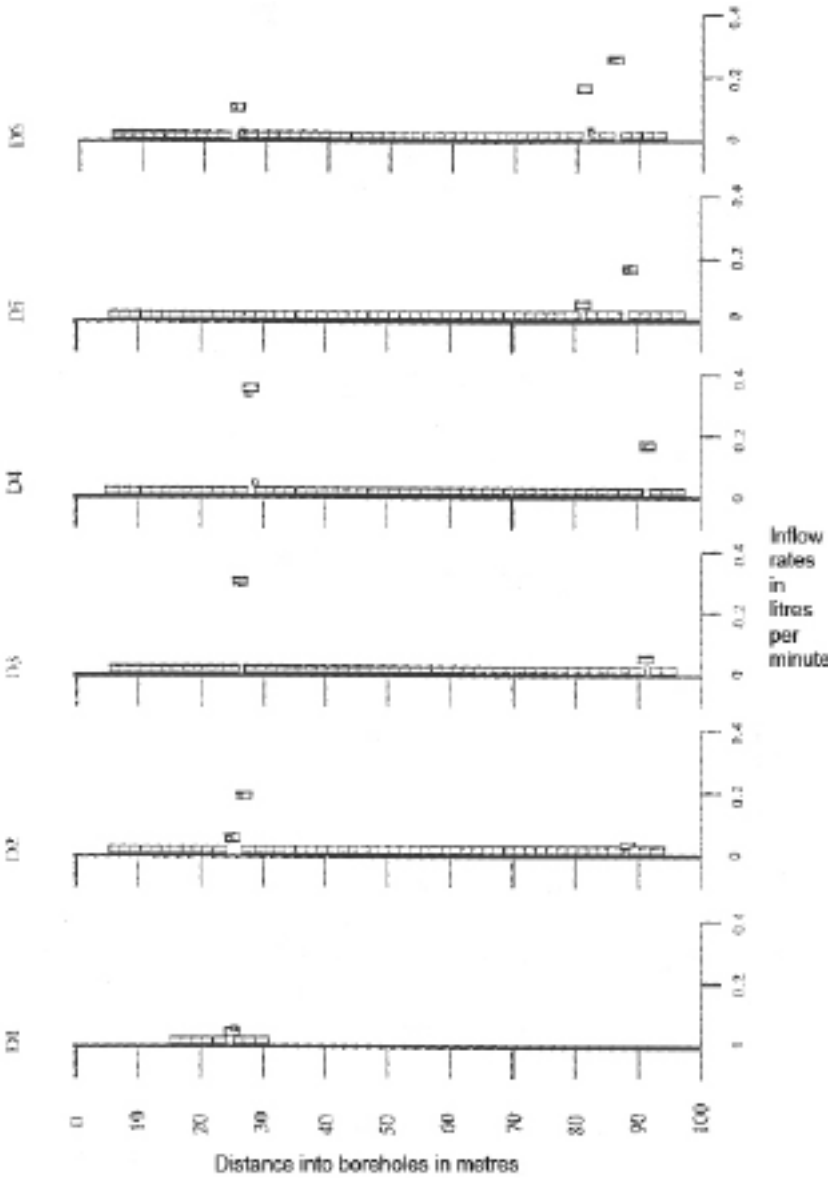

Figure A1-2. *Inflows along the 'D' boreholes during the SDE 'Step 3' (i.e. 210 m drawdown). NB inflow to D3 '90 m zone' has been included on the figure and removed from Figure A1-1.*

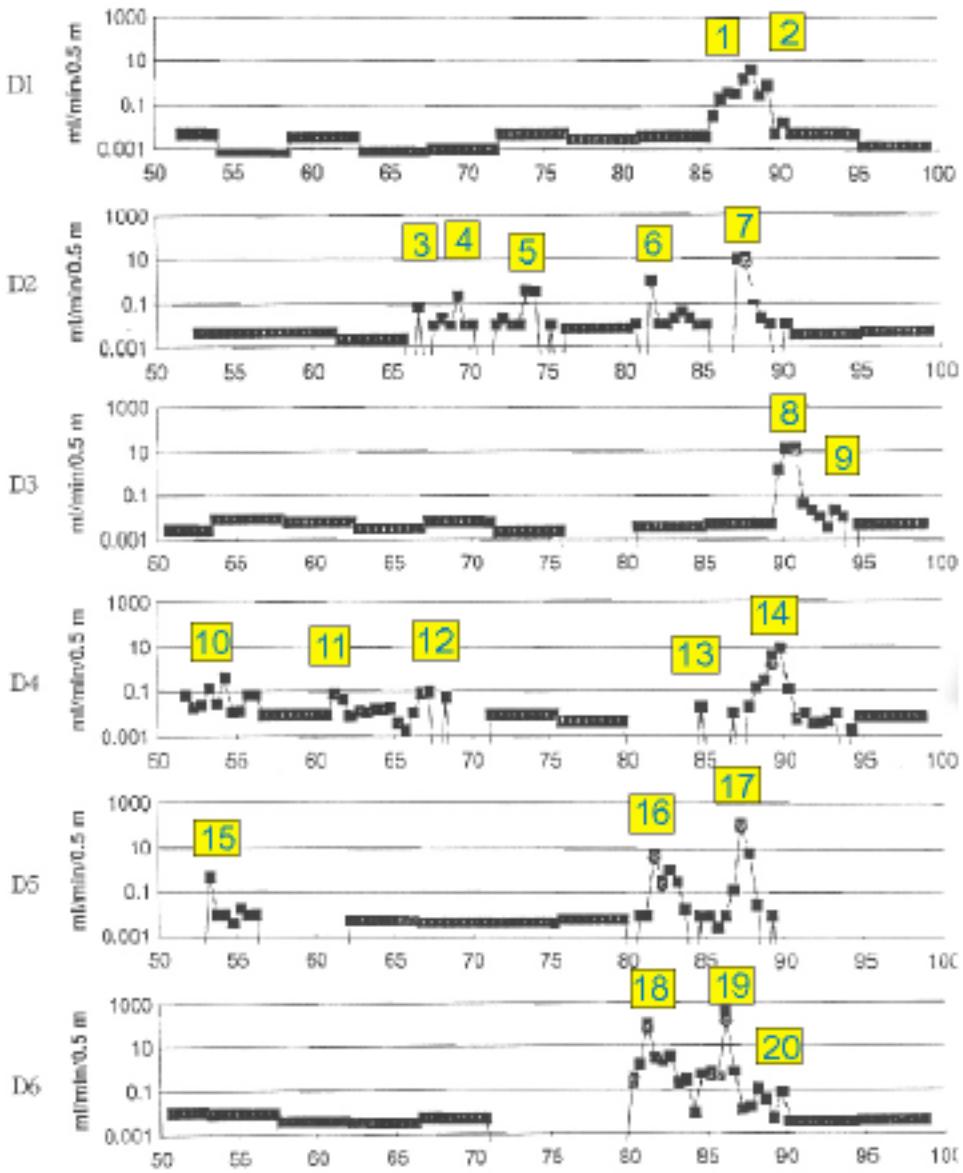

Figure A1-3. *Inflows to the 50 m of D boreholes remaining after the excavation of the validation drift. Note the extreme 6 decade logarithmic Y axis for flow rate. Diagram is taken from /Harding and Black 1992/. Inflow point numbering has been added by the authors of this report.*

The second very useful data set for the purposes of identifying the number or density of inflow points is that relating to the inflows collected in 'ceiling sheets' and 'floor sumps' within the 'Validation Drift'. Results are given in /Harding and Black 1992/, for two specific times after excavation (see Figure A1-4). The main facet of the results is the concentration of inflow to a small number of areas and the domination of inflow by one inflow that accounted for 49% of total inflow after 200 days.

The 50 m of drift had an internal surface area of about 440 m^2 of which approximately 62 m^2 was described as 'wet rock', or 14% of the surface area.

As a general observation, looking at the 'patches' of inflow in Figure A1-4, 6 or 7 inflow 'points' would appear to be a reasonable estimate. The 'Simulated Drift' could be estimated as having 20 inflow points in 50 (group) metres whereas the 'Validation Drift' probably had about 6 in the same length.

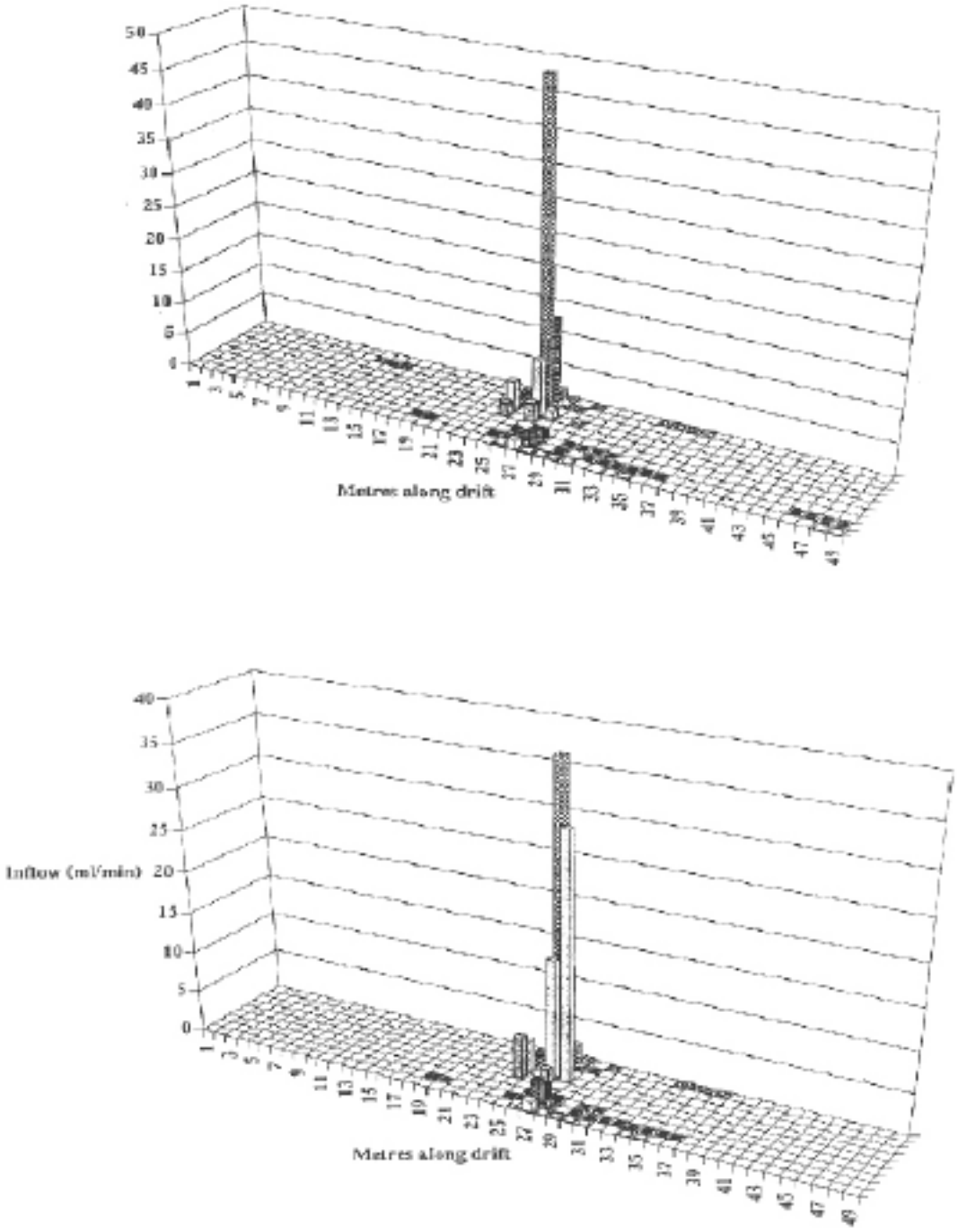

Figure A1-4. *Inflows to the Validation Drift for 5,000 hours (208 days) and 9,500 hours (396 days) after excavation. The surface of the drift was divided into 9 sectors, number 1 straddling the ceiling centre line, numbers 5 and 6 either side of the floor centre line. The 'ceiling sheets' (numbers 1, 2, 3, 8 and 9) are shaded blue in the diagram.*

A.2 Measurement of 'skin' and large-scale hydraulic conductivity

Both the Simulated Drift and the Validation Drift inflow experiments were observed in monitoring zones in nearby boreholes. Radial boreholes from the drift were omitted because of fears that they might participate directly in flow towards the Validation Drift so head measurements were performed in rather long monitoring zones, aligned at random angles to the D boreholes/Validation Drift system. This was far from ideal and also meant that

there were very few observations close to the 'cylinder' of discharge. The results for the Simulated Drift are ambiguous. At first glance, they show a very large skin, in the order of 80 m, which is even larger than the nearby Ventilation Drift (See Figure A1-5). However, the 80 m value is based on extrapolating the drawdown back to the circumference of the 'imaginary' Simulated Drift. If the extrapolation is continued then the full drawdown value is intersected at a similar value to the radius of a single 'D' borehole. In other words no skin at all. Using the actual radius of the central borehole, 37.5 mm, actually yields a slightly negative value of skin of about 20 m indicating that the D borehole configuration yields an effective radius larger than a single borehole but probably not as much as the full circumference of the Validation Drift. Given the uncertainties in the measurement point locations and the error involved in extrapolating back to the centre of the array from remote locations, it is dangerous to over-interpret the results.

The slope of the straight line in Figure A1-5 can be used to interpret a value for the bulk rock hydraulic conductivity based on measuring inflow and assuming cylindrical flow geometry. This yields a value of K = ~ 2E–9 m s^{-1} based on an inflow rate of 1.7 l/min (2.8E–5 m^3s^{-1}). This should be a 'large-scale' value and should be compared to the value from the Macro-Permeability test of ~ 1E–10 m s^{-1} obtained using the same method but using observation points closer to the abstraction system.

The Validation Drift shows a similar response to the Simulated Drift even though the total inflow is 1/16 of that for the Simulated Drift and the inflow configuration is only half the length (Figure A1-6). In this case however, there is definitely a positive skin of about 120 m. When combined with an inflow rate of 0.1 l/min (1.7E–6 m^3s^{-1}), this yields a value of bulk hydraulic conductivity of ~ 3E–10 m s^{-1}.

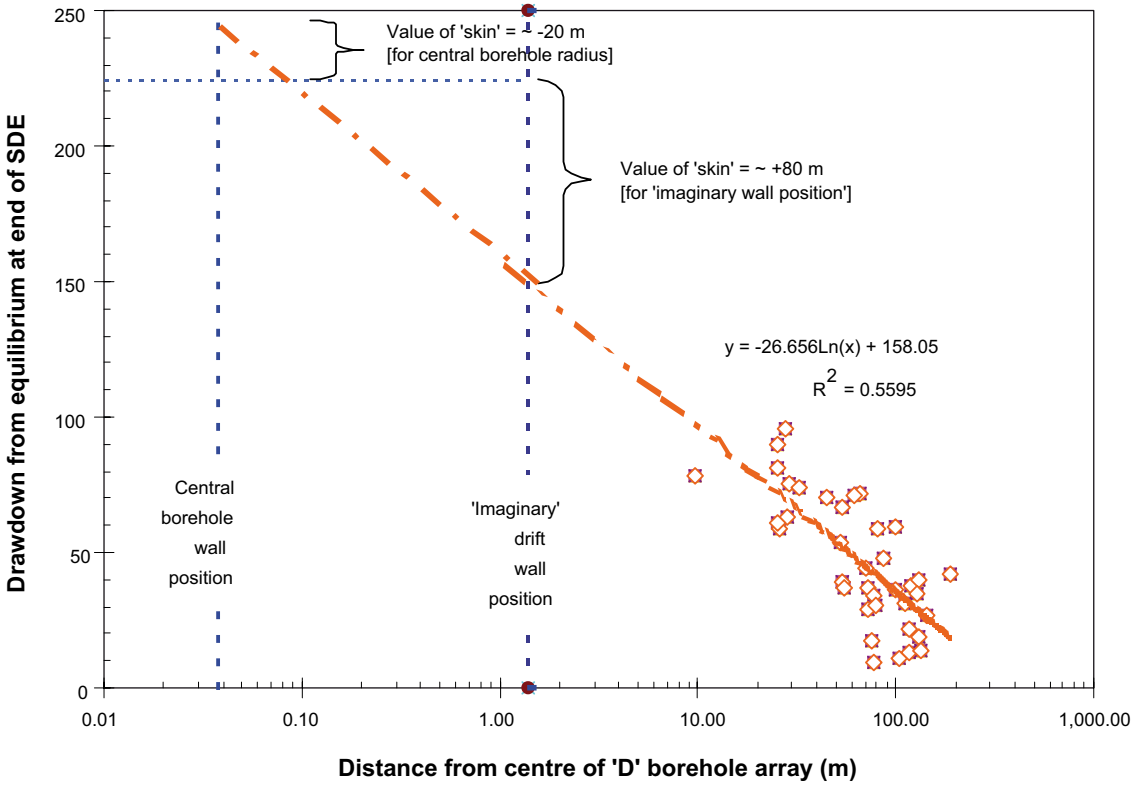

Figure A1-5. *Plot of head versus the logarithm of distance for the active monitored zones at the end of the Simulated Drift Experiment. NB the measurements are plotted at the mid point location of each measurement zone, some of which are tens of metres in length.*

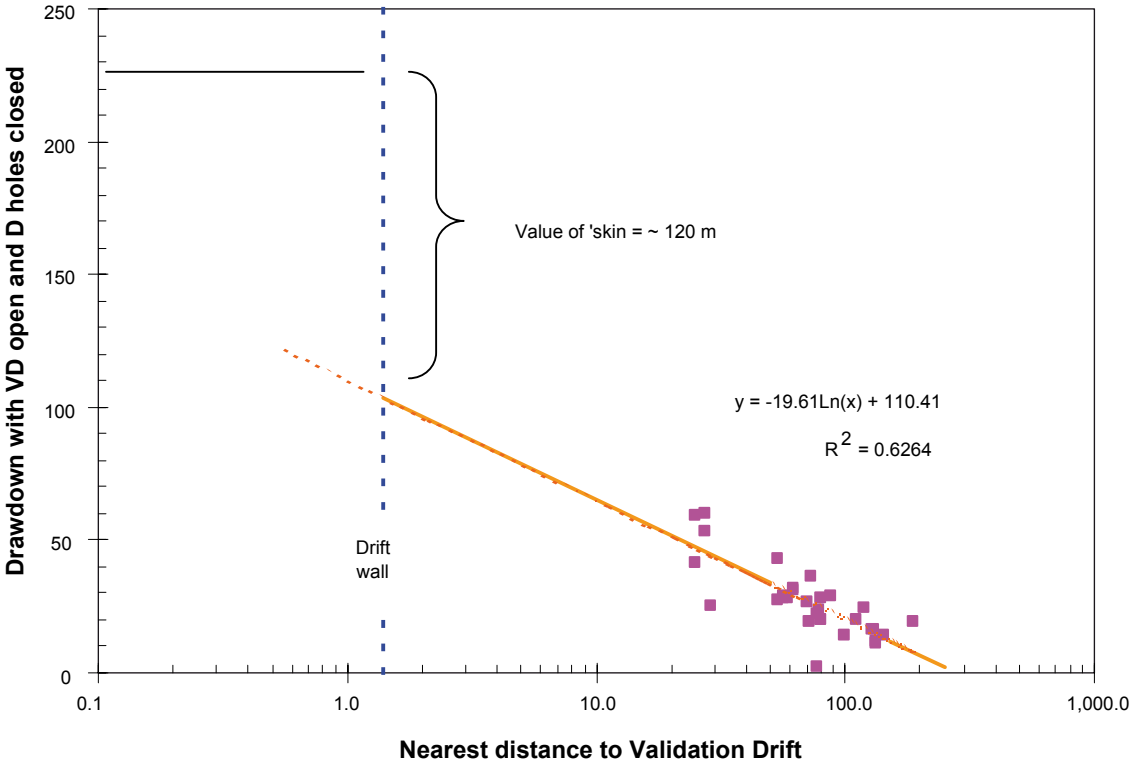

Figure A1-6. *Plot of head versus the logarithm of distance for the active monitored zones at the end of the Validation Drift Experiment.*

One final aspect of interest concerned the excavation of the Validation Drift which effectively converted the Simulated Drift configuration into the Validation Drift. Virtually as soon as blasting began the heads in the vicinity began to gradually recover. They continued rising steadily showing no signs of stopping at weekends when blasting was not undertaken. In other words, the skin and its associated reduction of inflow grew gradually and was not a direct effect of each blast round. This points to a hydraulic rather than a mechanical cause of the skin.

In summary, there was an observable positive skin at the end of the experimental period that surrounded the excavated Validation Drift. It seemed larger than that surrounding the 'Ventilation Drift' of the much earlier but nearby experiment. The situation is far more uncertain concerning the array of boreholes comprising the Simulated Drift. The most likely interpretation is that the array of boreholes set on the circumference of a 2.4 m diameter circle around a central borehole 'appeared hydraulically' like a single central borehole of slightly larger than drilled-diameter, a single borehole with a negative skin.

Ambiguity also concerns the interpretation of large scale hydraulic conductivity. The two open drift experiments, the Validation Drift and the Macro-Permeability experiment both yielded values of large scale hydraulic conductivity of about 2E–10 m s^{-1}. The borehole array experiment , the Simulated Drift, returned an interpreted value about 10 times larger from more-or-less the same measurement points as the Validation Drift. Since the large-scale hydraulic conductivity had not been altered in the meantime, this is a surprising result.

Appendix B

Implementation of a sparse channel network as a code plus viewer

B.1 Introduction

The approach described is implemented in a small Quintessa code, HyperConv. There is an associated viewer called LatticeViewer.dll that HyperConv can call.

B.2 Hyperconv

HyperConv is a console application that takes input from a text file. It can be run from a command prompt, e.g. HyperConv input.txt, or by dropping the input file onto the exe in Windows explorer. Alternatively, the exe can be launched and will prompt for the input file name.

The input file has a simple keyword-driven format. Each input line has a keyword (in capitals) followed by the associated value. The order is not important. Most inputs are required, but some have defaults. The table below lists the keywords.

Keyword and value	Description	Default
NX n	number of lattice nodes in X direction (i.e. along tunnel length)	–
NY n	number of lattice nodes in Y direction	–
NZ n	number of lattice nodes in Z direction	–
DX val	lattice spacing in the x-direction (m)	–
DY val	lattice spacing in the y-direction (m)	= DX
DZ val	lattice spacing in the z-direction (m)	= DX
TUNNEL_RADIUS val	radius of the tunnel (placed at the centre of y, z range along full x length) (m)	–
OUTER_RADIUS val	radius for outer boundary (from tunnel axis) (m)	to nearly reach the y and z boundaries
P_NEW prob	probability of a new channel starting after a bond that is not present	–
P_AGAIN prob	probability of a channel continuing to the next bond	–
CONDUCTIVITY_LOG_SD val	standard deviation of $\log_{10}$ of leg conductivity values	–
ROCK_CONDUCTIVITY_TARGET val	target conductivity for the rock as a whole (m/s)	–
CONDUCTIVITY_PERSISTS	indicates that channels have a single conductivity along their length	false
HEAD_DIFFERENCE val	difference between head at outer boundary and in tunnel	200
SEED n	initial random number generator seed	987654321
NUM_REALISATION n	number of realisations	1
VIEWER ON/OFF	indicates if viewer is used (only for first realisation)	ON if one realisation, OFF otherwise
LOG_FILE filename	for copy of key inputs and results	none
TUNNEL_FILE filename	for list of flows by position on tunnel wall	none
HEAD_FILE filename	for list of heads versus radius	none

An input summary is echoed back to the console and for each realisation; the seed is reported, followed by the number of active nodes and channels. As the flow is calculated, the iterative convergence is reported. The total vertical flow and derived K_{rock} are reported. Then the tunnel flow and derived h_{skin} and K_{rock} are reported using the various approaches described above. This same information is written to a log file if requested.

The optional tunnel output file has individual tunnel flow values at each position. The optional head output file has the heads and radius values. The log file ends with a summary of the results of all realisations suitable for importing into Excel for further analysis. The code has been run successfully on lattices up to 100×100×100.

B.3 Lattice viewer

The Lattice Viewer is launched automatically by HyperConv if requested. Various results can be viewed on the lattice:

- CSs shows all the channels coloured by the C_S (specific conductivity);
- Active CSs shows only the connections that are linked to the tunnel and outside including those in the tunnel or outside;
- Relevant Active CSs omits those in the tunnel or outside;
- Log10(Relevant Active CSs) is the same but coloured as a log10 value;
- Heads shows the average head on each relevant active bond;
- Flows show the absolute flow rates on each relevant active bond;
- Log10(Flows) shows the $\log_{10}$ of the absolute flow rate, with zero flows not drawn.
- In each case, a key is shown. A rainbow colour scheme is used, with blue at the low end and red at the high end.
- Set Projection allows the view to be changed. The eye position and point being looked at can be changed. The up direction can also be changed, but should usually be left as it is.
- With a right mouse click, Show Range… and Clear Range is available. These allow the setting and clearing of the range of values displayed. The colour map can be set to use the reduced range or the full range.

Various keyboard keys perform functions. Single slices can be displayed using ‘x’, ‘y’ or ‘z’ – and the particular plane can be changed with the up and down arrows. Holding the ‘ctrl’ key with the arrows allows multiple slices to be displayed. The ‘b’ key toggles display of the bonds between the slices displayed. The ‘a’ keys resets to showing all the lattice.

Appendix C

Possible future studies

C.1 Introduction

As is inevitable in a pilot study of this kind, many more questions have been raised than could be tackled in this project. These are discussed here, with suggestions as to how they might be carried forward. They are divided broadly into three groups relating to the following aspects,

- The meaning of fundamental parameters as applied to channel network systems.
- Understanding how the channel network numerical model behaves.
- Understanding field experiments.

C.2 The meaning of fundamental parameters as applied to channel network systems

The meaning of flow dimension within a channel network system. This could be assessed by constructing homogeneous networks based on a single inflow point and measuring all distances in proper relationship to the inflow point in a spherical flow system.

The work reported here calculates four values for hydraulic conductivity of a sparse channel network and contains a fifth, the target conductivity. The relationships between them need to be resolved.

The basic model calculates a ‘face-to-face’ K. This needs to be investigated further in case there is a ‘skin effect’ on the faces of the model. This could be achieved by sampling head within the model rather than assuming that the face heads are transmitted within the model without any effective hyper-convergence. The relationships between the specified conductances and the overall hydraulic conductivity needs to be understood better.

C.3 Understanding how the channel network numerical model behaves

The basic model relies on a lattice whose spacing has to be specified. The basis for choosing this separation is not entirely clear. Observations of the spacing between flowing features in boreholes and on tunnel walls clearly provide some information on channel separation, but this is convoluted with the probability that a channel is flowing. Observations on all potential channels could be used, but this raises questions on how these could be observed.

Channels can only intersect in the lattice if they lie on a common plane. Thus, channels can pass near to each other (one lattice spacing apart) without interacting. The generation algorithms could be encouraged to generate more channels in some planes to enhance the intersection probabilities. A simple experiment with this type of modification was tried in the current project; this suggested that any such “encouragement” should not extend across the whole domain, but rather be localised to represent fracture planes where channels occur.

No attempt has yet been made to look at borehole intersections. Some rule will be needed to decide whether a channel connects to a borehole. This could be based on geometry alone (by giving the channels a width) or on a vaguer notion of a probability of connection as a function of distance between the channel centreline and the borehole.

Channel length and specific conductance are currently independent. It is commonly assumed that larger features in terms of length are also larger in terms of aperture, so a correlation could be introduced to represent this.

The possible effects of tunnel wall desaturation have not yet been included. It was initially thought that this might be necessary to see any skin effect, but this proved not to be the case. If desaturation effectively prevents flow into the tunnel for some channels then it might reduce the apparent connectivity and so reinforce the skin effect.

The outer boundary condition is at an arbitrary distance and the assumption that the head is uniform at this distance is at odds with the behaviour of the system itself. Other options for treating the extremities of the model system need to be looked at.

Lattice bonds that are not included in channels are currently omitted entirely. They could be given a background conductance, e.g. to simulate the conductivity of smaller scale features.

The length distribution of channels could be generalised from the current geometric distribution.

The impact of the variability in the specific conductance has not yet been explored. Also, intermediate choices of correlation length within a channel might be useful (currently either the whole channel has the same value or every bond differs).

- What controls the sign and size of the skin effect?
- What controls the calculated conductivity from the tunnel?
- Should the head v log r algorithm be restricted to a certain distance from the tunnel?

Some measures of connectivity need to be developed, such as average number of connections per channel, fractions of channels that are flowing, etc. These might provide predictors for the skin and conductivity results.

C.4 Understanding field experiments

This report contains an idea for understanding the SD/VD experiments at Stripa. The idea should be tested in a model together with different spacings and locations for the parallel boreholes that are thought to provide the extra channel performance. This would be a project in itself since it opens up the possibility of new ways to organise site investigations so as to provide defining data on fractured rock groundwater systems suspected of being sparse channel networks.

Single borehole hydraulic tests have long been used to investigate fractured rocks. One of the obvious questions is how long should a test interval be and what is the value of knowledge of the location and transmissivity of individual fractures if they form part of a channel network rather than a network of essentially 2 dimensional features (i.e. fractures). How can channel networks be reconstructed from field data? What is the value of the single borehole connectivity test?

- What are the implications of sparse channel network geometry on tracer tests?